Modeling Food Webs: Exploring Unexplained Structure Using Latent Traits

Rudolf Philippe Rohr,[1,*] Heike Scherer,[2] Patrik Kehrli,[1,†] Christian Mazza,[3] and Louis-Félix Bersier[1]

1. Unit of Ecology and Evolution, University of Fribourg, Chemin du Musée 10, 1700 Fribourg, Switzerland; 2. Department of Mathematics, University of Geneva, 2–4 rue du Lièvre, 1211 Geneva, Switzerland; 3. Department of Mathematics, University of Fribourg, Chemin du Musée 23, 1700 Fribourg, Switzerland

Submitted November 2, 2009; Accepted April 8, 2010; Electronically published June 11, 2010

Online enhancements: appendix, zip file.

abstract: Several stochastic models have tried to capture the architecture of food webs. This approach is interesting, but it is limited by the fact that different assumptions can yield similar results. To overcome this limitation, we develop a purely statistical approach. Body size in terms of an optimal ratio between prey and predator is used as explanatory variable. In 12 observed food webs, this model predicts, on average, 20% of interactions. To analyze the unexplained part, we introduce a latent term: each species is described by two latent traits, foraging and vulnerability, that represent nonmeasured characteristics of species once the optimal body size has been accounted for. The model now correctly predicts an average of 73% of links. The key features of our approach are that latent traits quantify the structure that is left unexplained by the explanatory variable and that this quantification allows a test of whether independent biological information, such as microhabitat use, camouflage, or phylogeny, explains this structure. We illustrate this method with phylogeny and find that it is linked to one or both latent traits in nine of 12 food webs. Our approach opens the door to the formulation of more complex models that can be applied to any kind of biological network.

Keywords: biological network, latent variable, statistical model, body size, phylogeny, community structure.

Introduction

Understanding food-web structure remains one of the central questions in ecology, and it is of both fundamental and practical relevance. Cohen (1977) pioneered this research by assembling a collection of webs and analyzing regularities in their structures. This statistical approach was based on derived descriptors (e.g., proportions of top, intermediate, and basal species, connectance, intervality; Sugihara et al. 1989; Cohen et al. 1990; Bersier et al. 2002), which were typically regressed with regard to food-web size as measured by number of species. Stochastic and probabilistic models of food-web architecture were proposed to account for the observed relationships (Cohen and Newman 1985; Williams and Martinez 2000; Drossel et al. 2001; Cattin et al. 2004; Rossberg et al. 2006; Allesina et al. 2008; Petchey et al. 2008). The goodnesses of fit of these models were evaluated by comparing observed and predicted values of derived descriptors (with the notable exception of the model by Allesina et al. [2008], who used a likelihood approach to compute the probability of reproducing the entire web).

The aim of these models was to uncover the major factors underlying food-web organization. In almost all cases, a hierarchy was assumed to exist between the species that was described by a rank or a niche value. Two nonexclusive factors have been proposed to generate the hierarchy: body size, and phylogeny. In Cohen and Newman's (1985) pioneering cascade model, a species with a given rank is allowed to eat any species of lower rank, with a given probability. The other models are built on this general framework, usually with the number of species and the total number of trophic links as parameters. Earlier models (cascade: Cohen and Newman 1985; niche: Williams and Martinez 2000; nested hierarchy: Cattin et al. 2004) differ only in the rules used to assign the trophic links between consumers and resources. Later approaches involved more parameters to improve the quality of the models. Rossberg et al. (2006) introduced a dynamical stochastic model for food-web structure that had five free parameters. In that model, each species is characterized by the log of its body size and two binary vectors: the foraging traits and the vulnerability traits. These behavioral traits do not correspond directly to measurable quantities; they are latent parameters. These traits and the number of species evolve over time by speciation, extinction, and adaptation. Drossel et al. (2001) developed a model where

* Corresponding author; e-mail: rudolf.rohr@unifr.ch.

† Present address: Station de Recherche Agroscope Changins-Wädenswil, 1260 Nyon, Switzerland.

Am. Nat. 2010. Vol. 176, pp. 170–177.
DOI: 10.1086/653667

population dynamics are explicitly modeled and determine extinctions. Again, they introduced for each species a latent trait ("features of species") that controls trophic interactions. Recently, Petchey et al. (2008) introduced a mechanistic model. This was the first attempt to predict the actual links in real trophic matrices as opposed to simply generating plausible webs with a stochastic model. The body-size distribution was used to predict feeding interactions on the basis of allometric rules and optimal foraging theory. It showed that body size plays an important role in trophic relations, but the authors also pointed out that a second trait would be required to better explain the structure of the predation matrix.

In this article, we propose a purely statistical approach to explore the structure of food webs. This approach is inspired by the methods used in social-network studies (Hoff 2009). We define and investigate two models: the body-size model and the latent-trait model. The former uses the prey-over-predator body-size ratio as the explanatory variable. We show that, with this model, a large part of the variability remains unexplained. In the second model, our aim is to quantify the part that is not explained by the first model. For this purpose, we introduce latent variables—one vulnerability trait and one foraging trait—for each species (Rossberg et al. 2006). Even though these abstract latent traits are not directly observable, we are able to estimate them from the predation matrix and the body sizes of the species by using Bayesian statistics and Markov Chain Monte Carlo (MCMC) techniques. Finally, we show that these latent variables are very useful to test whether biological information other than body-size ratios plays a role in determining the architecture of the food web.

Material and Methods

The predation matrix is the matrix $\{a_{ij}\}$, which is defined by $a_{ij} = 1$ if j consumes i and $a_{ij} = 0$ otherwise. The aim of our statistical models is to fit the predation matrix of a food web. We achieve this in the following manner:

1. For each pair of species (i, j), we estimate the linking probability $\Pr(a_{ij} = 1)$ using the model.
2. We compute the expected number of trophic links $\hat{L} = \sum_{ij} \Pr(a_{ij} = 1)$.
3. The fitted predation matrix is obtained by attributing trophic links to the $\hat{L}$ pairs of species having the highest linking probabilities.

From a statistical point of view, the attribution of trophic links is a binary classification problem. In this situation, a frequently applied method is the logistic regression. Thus, the equations for the models are given for the logit of $\Pr(a_{ij} = 1)$, that is, $\log[\Pr(a_{ij} = 1)/\Pr(a_{ij} = 0)]$.

Body-Size Model

Our body-size model uses the log ratio of the body sizes of resources over those of consumers (equivalently, the difference in the log body sizes) as the explanatory variable (Brose et al. 2006; Petchey et al. 2008). In order to implement the idea of an optimal size range for the prey, we model the logit of the linking probability in the following manner:

$$\log\left[\frac{\Pr(a_{ij} = 1)}{\Pr(a_{ij} = 0)}\right] = \alpha + \beta \log\left(\frac{m_i}{m_j}\right) + \gamma \log^2\left(\frac{m_i}{m_j}\right).$$

The parameters to be estimated are α, β, and γ. The quadratic polynomial in the log body-size ratio for the logit creates a curve for the linking probabilities whose general aspect resembles a Gaussian distribution function. The bell shape reflects the idea of an optimal range for the prey, consistent with niche theory. In this respect, the optimum (in difference of log) is given by $-\beta/2\gamma$, and the ecological range (standard deviation in difference of log) is approximated by $(-1/2\gamma)^{1/2}$. As a typical example, figure 1*a* shows the estimated probabilities for the body-size model in red and the values of the observed predation matrix in blue as functions of the log body-size ratios. The dashed line indicates the threshold above which we attribute the trophic links.

Latent-Trait Model

Since the body-size model typically predicts only a low percentage of trophic links, we introduce latent terms to quantify the part that is not explained by the optimal body-size ratio. The most general way to do this is to summarize the unobserved part into a matrix **M**, that is,

$$\log\left[\frac{\Pr(a_{ij} = 1)}{\Pr(a_{ij} = 0)}\right] = \alpha + \beta \log\left(\frac{m_i}{m_j}\right) + \gamma \log^2\left(\frac{m_i}{m_j}\right) + M_{ij}.$$

The matrix **M** can be understood as an analog of the residuals in a Gaussian framework. At this point, one could be tempted to try to estimate the components of **M** directly, but since the number of parameters exceeds the number of observations, this would not be reasonable. Note also that each component of **M** refers to a trophic interaction (present or absent) between two species. A better approach is to find a structure where the latent terms refer not to pairwise interactions but to species, which allows a biological interpretation. This can be achieved

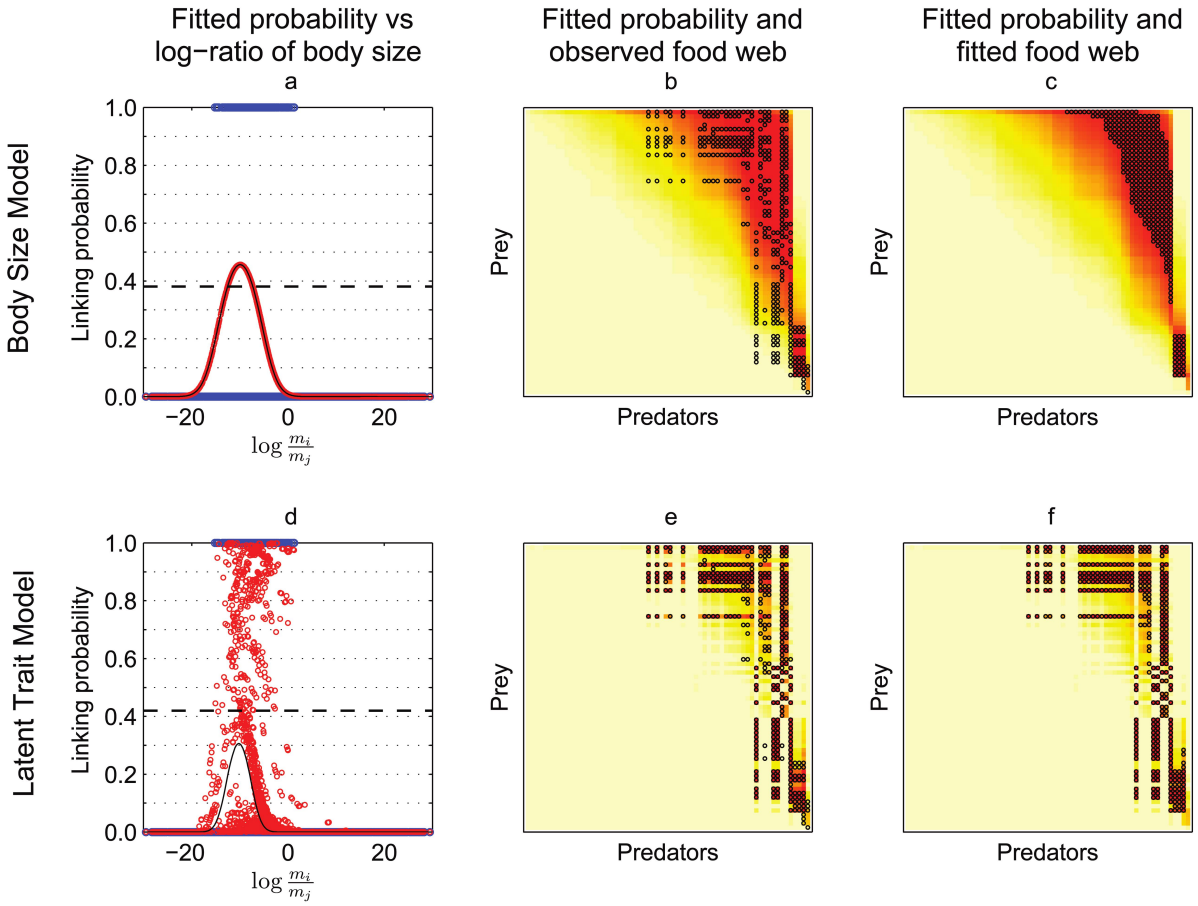

Figure 1: Comparison of the body-size model and the latent trait model for the Tuesday Lake food web. In *a* and *d*, with respect to log body-size ratio, the values of the observed predation matrix are shown in blue and those of the fitted linking probabilities are shown in red (note that these are individual points corresponding to the 66^2 possible pairs of species). The black curve illustrates the part of the fitted linking probability contributed by the body-size term of the corresponding model. The dashed line indicates the threshold above which the fitted linking probabilities are interpreted as trophic links. *b* and *e* show the observed predation matrix (with the 66 species ordered from smallest to largest on both axes), where the black circles represent trophic links. The background color illustrates the magnitudes of the corresponding predicted linking probabilities, increasing from pale yellow to red. *c* and *f* show again the magnitudes of the fitted linking probabilities, now overlaid with the fitted predation matrix.

using singular-value decomposition (SVD) and concentrating only on the most explicative singular value (see "Singular-Value Decomposition (SVD)" in the online edition of the *American Naturalist*). With this approach, the matrix **M** has the structure $M_{ij} = v_i \delta f_j$, where δ is the maximal singular value, v_i (where $i = 1 \ldots S$) refers to a species as prey, and f_j (where $j = 1 \ldots S$) refers to a species as predator. Accordingly, our latent-trait model is

$$\log\left[\frac{\Pr(a_{ij} = 1)}{\Pr(a_{ij} = 0)}\right] =$$

$$\alpha + \beta \log\left(\frac{m_i}{m_j}\right) + \gamma \log^2\left(\frac{m_i}{m_j}\right) + v_i \delta f_j.$$

Each species i is now characterized by three numbers: the known body size m_i and the unknown latent traits v_i and f_i, which we call vulnerability and foraging, respectively. These are estimated from the observed predation matrix during the fitting of the model. The introduction of the latent-trait term allows noncontiguous diet ranges so that, as in nature, predators are not constrained to feed on all prey within a continuous region of the body-mass axis. In this case, a large positive latent-trait term (the product $v_i \delta f_j$) can compensate for an unfavorable body-size ratio, whereas a negative latent-trait term can produce a low linking probability even if the body-size ratio is favorable. In figure 1*d*, the estimated linking probabilities are depicted in red as a function of the log ratio of body size.

The black curve represents the effect of body size, corresponding to the quadratic polynomial in the logit function. It is clear that the contribution of the latent traits to the linking probability is very important.

Variants of the Latent-Trait Model

We have also considered the following subcases of the latent-trait model: (1) a model with latent traits only, that is, $\log[\Pr(a_{ij} = 1)/\Pr(a_{ij} = 0)] = v_i\delta f_j$; (2) a model with the latent trait of vulnerability only, that is, $M_{ij} = v_i\delta$; and (3) a model with the latent trait of foraging only, that is, $M_{ij} = \delta f_j$.

Parameter Estimation

The body-size model is a generalized linear model (GLM) with explanatory variables $\log(m_i/m_j)$ and $\log^2(m_i/m_j)$. Thus, we estimate α, β, and γ by using a GLM-fitted algorithm based on maximum likelihood with logit linking function and binomial distribution. For the latent-traits model we estimate the parameters α, β, γ, and δ, and for each species we estimate the two latent traits. It is important to understand that the latent traits and δ cannot be estimated from the residuals of the body-size model but instead must be fitted simultaneously with α, β, and γ. We achieve this using a Bayesian approach and an MCMC technique (see "Estimation of the Parameters with Markov Chain Monte Carlo (MCMC) Techniques" in the online edition of the *American Naturalist*).

Interpretation of Latent Traits

A priori, we can interpret the latent traits in two ways: mathematically, as their product, or biologically, as their distance. Latent traits are introduced in the model in terms of their product, $v_i\delta f_j$. Thus, a positive term (implying that v_i and f_j are both of the same sign) increases the probability of the existence of a trophic interaction between i and j (relative to the optimal ratio part), and vice versa. Reasoning in terms of distance allows a separate interpretation of foraging (or vulnerability) traits: if two species j and k have similar foraging traits—more precisely, if $|f_j - f_k|$ is small—then for any given potential prey i, the term $v_i\delta f_j$ is close to the term $v_i\delta f_k$. For consumers j and k, the contribution of the latent term to the linking probability is of similar magnitude, that is, there should be similarities in their predation behavior. The same reasoning applies to the vulnerability traits. Thus, our latent traits can be used to quantify the similarities between species in their roles of predator and prey, with the key characteristic that the effect of the optimal body-size ratio is removed. A posteriori, we can of course try to understand whether the values of latent traits can be interpreted directly.

How to Relate Latent Traits to Biological Information

As latent traits quantify the similarity between species, a sensible approach to relate them to external information is to compare similarity matrices. A standard method is the Mantel test (Sokal and Rohlf 2001), which can be used to detect whether there is a correlation between similarity matrices on the basis of latent traits and the biological descriptors of interest. Here we demonstrate this technique with (1) trophic structure, (2) body size, and (3) phylogeny. The first comparisons are used as a test to assess whether our latent traits capture the corresponding information of the food-web matrix. The second comparisons test whether there remains an effect of body size that is not accounted for by the optimal ratio. Finally, the third comparison uses the latent traits to test whether evolutionary history contributes to food-web architecture when the optimal ratio has been removed.

For the foraging latent traits, we first compute the distances $d_{ij} = |f_i - f_j|$. The coefficients of the corresponding similarity matrix are $1 - d_{ij}/\max_{ij} d_{ij}$. The similarity matrix with respect to the vulnerability traits is computed in the same manner. We use the Jaccard index (Jaccard 1908) to describe trophic similarity, separating foraging, and vulnerability. Trophic similarity with respect to foraging between two species i and j (Jaccard foraging) is the number of common prey divided by the total number of prey of the two species. Similarly, the Jaccard index with respect to vulnerability between species i and j (Jaccard vulnerability) is the number of common predators divided by the total number of predators of the two species. Similarity in body size is computed in the same way as for latent traits. The phylogenetic similarity between two species i and j is computed by assigning values to taxonomic levels from 1 (phylum) to 17 (genus) and dividing the value of most precise common taxonomic level by 1 plus the value of the most precise level to which either of the two species was determined (Cattin et al. 2004).

We use Spearman's rank correlation coefficient in the Mantel tests since it is less sensitive to outliers than Pearson's coefficient. When comparing phylogenetic similarity and similarity with respect to latent traits, it is important to note that the two types of similarity matrices contain body-size information (see "Results and Discussion"). In order to compare them independently of common body-size components, we use a partial Mantel test; that is, before comparison, we first remove the linear correlation of body size from both the latent-trait and the phylogenetic-similarity matrices.

Data

We used the published data set of Brose et al. (2005), from which we extracted 12 highly resolved food webs: (1) Silwood Park (Cohen et al. 2005), (2) grassland (Dawah et al. 1995), (3) Sierra Lakes (Harper-Smith et al. 2005), (4) Tuesday Lakes (Jonsson et al. 2005), (5) Mill Stream (M. E. Ledger, F. Edwards, and G. Woodward, unpublished data), (6) Broom (Memmott et al. 2000), (7) Celtic Sea (Pinnegar et al. 2003), (8) Mulgrave River (T. S. Rayner, unpublished data), (9) Goettingen (Ulrich 1999), (10) Skipwith Pond (Warren 1989), (11) Sheffield (P. H. Warren, unpublished data), and (12) Broadstone Stream (Woodward et al. 2005). We discarded webs for which trophic interactions were not determined from direct observations, as well as, for computational reasons, one very large web. Detailed information is presented in table A1, which is available in a zip file in the online edition of the *American Naturalist*.

Results and Discussion

Goodness of Fit

We fitted the body-size model and the latent-trait model to 12 high-quality food webs. In order to compare the performance of the two models, we computed as a first criterion the proportion of correctly predicted trophic links (table 1; Petchey et al. 2008). It is clear that the latent-trait model performs much better than the body-size model. The observed and predicted connectance values for the 12 food webs are listed in table 1. Both models performed almost equally as well with respect to the fitted connectance, and in only one case did the body-size model predict a slightly different value. That the latent-trait model outperforms the body-size model is not surprising, as it involves $2S + 1$ more parameters. However, in 10 of the 12 food webs, the Akaike Information Criterion (AIC) was lower for the latent-trait model than it was for the body-size model (table 1). This confirms that the addition of the $2S$ latent traits is justified by the considerable gain in accuracy.

Figure 1 allows for visual comparison of the quality of the fit of the two models for the Tuesday Lake food web. One can easily see that the body-size model poorly reproduces the structure of the food web. Figure 1*f* shows that the magnitudes of the fitted probabilities from the latent-trait model closely follow the structures of the real predation matrix and that noncontiguous diets are permitted. The corresponding figures for the 11 other food webs are available in a zip file in the online edition.

We computed variants of our latent-trait model: one with latent traits only (without information on body size), one with body size and the vulnerability trait only, and one with body size and the foraging trait only. Table 2 gives the results for these variants and reveals that they never outperformed the original latent-trait model.

Additionally, we computed the predicted optimal $\log_e$ body-size difference and the ecological range representing an optimal diet range for both the body-size and the latent-trait models (table 1). We point out that for all food webs except 1, 2, and 9, the predicted optimal $\log_e$ body-size difference is negative, implying that predators are larger than their prey. Webs 1, 2, and 9 are parasitoid networks, and positive estimates are thus expected (Cohen et al. 2005). Web 2 is unusual in that the body-size ratio fails

Table 1: Results and goodness of fit of the body-size and latent-trait models

				Body-size model					Latent-trait model				
Food web	S	C	Body-size measure	$\hat{C}$	%	AIC	Optimum difference	Ecological range	$\hat{C}$	%	AIC	Optimum difference	Ecological range
1	34	4.8	Length	9.2	16	439	.1	.4	4.8	71	374	.0	.3
2	25	3.1	Length	3.1	2.9	913	…	…	3.1	44	944	…	…
3	37	14.0	Length	13.7	29	960	−4.3	3.2	14.0	93	337	−2.3	1.2
4	66	8.7	Mass	8.7	46	1,643	−9.9	3.3	8.7	87	873	−10.2	2.1
5	79	5.9	Mass	5.9	36	1,626	−20.8	5.6	5.9	74	1,358	−24.4	6.3
6	55	3.3	Length	3.3	12	873	−4.1	3.8	3.3	66	657	−4.5	14.6
7	57	6.3	Mass	6.6	19	1,223	−4.4	2.0	6.3	65	1,018	−5.2	2.1
8	62	5.5	Length	5.5	11	1,307	−6.0	2.6	5.5	64	1,010	−6.7	2.7
9	24	4.2	Mass	4.3	13	173	1.9	1.0	4.2	83	209	1.6	.7
10	67	7.8	Length	7.3	13	2,269	−1.4	1.2	7.8	67	1,491	−1.7	1.1
11	58	4.9	Length	5.1	6	1,276	−1.4	1.5	4.9	72	762	−3.9	1.8
12	29	18.6	Mass	18.5	36	736	−11.6	6.4	18.6	92	285	−5.9	3.1

Note: We report for each food web the number of species (S), the connectance (C), the body-size measure, the fitted connectance ($\hat{C}$), the proportion of correctly fitted links (%), the Akaike Information Criterion (AIC), the optimum difference in log body size, and the ecological range. The identifiers in the first column refer to those listed in "Data."

Table 2: Model comparison

Food	B.S. only		B.S. + L.T.		L.T. only		B.S. + vul.		B.S. + for.	
web	%	AIC	%	AIC	%	AIC	%	AIC	%	AIC
1	16	439	**71**	**374**	52	405	25	462	38	397
2	2.9	**913**	**44**	944	29	924	18	927	23	926
3	29	960	**93**	**337**	68	623	47	918	66	530
4	46	1,643	**87**	**875**	37	1,607	60	1,429	46	1,633
5	36	1,626	**74**	**1,358**	57	1,552	56	1,502	55	1,558
6	12	873	**66**	**657**	41	761	38	687	15	953
7	19	1,223	**65**	**1,018**	56	1,086	43	1,128	47	1,123
8	11	1,307	**64**	**1,010**	57	1,105	31	1,226	48	1,143
9	13	**173**	**83**	209	25	251	29	220	29	202
10	13	2,269	**67**	**1,491**	52	1,619	31	2,154	41	1,774
11	6	1,276	**72**	**762**	55	811	25	1,255	46	802
12	36	736	**92**	**285**	87	410	37	791	83	307

Note: For each model, we report the proportion (%) of correctly predicted trophic links and the Akaike Information Criterion (AIC). We consider the following models: the body-size model (B.S. only), the body-size model and the "original" latent-traits model (B.S. + L.T.), the model with the latent traits only (L.T. only), the model with body size and the latent trait of vulnerability only (B.S. + vul.), and the model with body size and the latent traits of foraging only (B.S. + for.). For each food web, the best value is bolded.

to totally explain interaction structure and no optimum can be estimated (see fig. A2, available in a zip file in the online edition).

Latent Traits

At this point, the key question is whether the addition of latent traits, which quantify the part of the variation not explained by the optimal body-size ratio, just introduces purely artificial terms or whether it represents a biologically meaningful and justified model improvement. Because the optimal ratio leaves a large part of the variation unexplained, one may expect that some correlation is left between the latent traits and the original information on vulnerability and foraging. The latter can be measured with Jaccard similarity.

We compared the similarity in latent traits to the Jaccard similarities with Mantel tests and found highly significant correlations in 21 out of 24 cases (see table A2, available in a zip file in the online edition). These simple tests confirm that the vulnerability and foraging latent traits are not just fitting parameters but also carry biologically relevant information, with the crucial feature that they are independent of an optimal body-size ratio. We can now use our latent traits to explore which independent biological factors should be added to the optimal ratio to better understand food-web structure.

Comparison with Body Size. Does the optimal-ratio term of the model capture all of the influence of body size on trophic behavior? In other words, is there a correlation between latent traits and body size? We performed Mantel tests between the similarity in body size and against the similarity in latent vulnerability and foraging traits, respectively. Table 3 shows that the optimal body-size ratio does not carry all of the information related to body size. It is interesting that the latent foraging traits are, in general, more closely related to body size than the vulnerability traits are.

Comparison with Phylogeny. Phylogeny has been suggested as a major factor underlying food-web architecture (Cattin et al. 2004; Bersier and Kehrli 2008). Mantel tests between phylogeny and latent-traits similarities resulted in six significant cases out of 12 food webs for the vulnerability traits and seven cases for the foraging traits (table 3). In all, latent traits were not correlated with phylogeny in only three webs, all of which are from freshwater habitats. Phylogeny and body size are not independent, so that the optimal body-size ratio may carry some phylogenetic signal. Finding a significant correlation indicates that phylogeny intervenes in the network in a manner independent from the optimal ratio. Apart from body size and phylogeny, other species characteristics could determine the probability of trophic interactions and could be analyzed in future work using latent traits, for example, microhabitat use, color and camouflage patterns, chemical and other defensive traits, or circadian activity.

Direct Interpretation of the Values of Latent Traits. In order to explore whether we can directly interpret the values of the latent traits, we plotted the estimated foraging traits versus vulnerability traits in figure 2 for the Goettingen food web (for the other webs, see figs. A1–A24 in the zip file in the online edition). We observed three general features: (1) all basal species have very similar foraging traits, whereas their vulnerability traits are more variable: the top predators show the opposite pattern, and the intermediate species generally have a high variability in both traits; (2) the higher the absolute value of the foraging trait, the higher the number of prey, and similarly for the number of predators and the vulnerability trait (see the three-dimensional figures in the zip file available in the online edition); (3) for almost all trophic interactions, the sign of the vulnerability trait of the prey is the same as the sign of the foraging trait of the predator. Their product is thus positive, yielding a positive contribution to the overall probability for a link. This indicates that a direct biological interpretation of latent traits must be performed with caution. For example, two prey characterized by a similar number of predators can have vulnerability traits of opposite sign (e.g., see species 30 and 35 in fig. A12 in the zip file available in the online edition).

Table 3: Results of the Mantel tests

	Body size versus latent vulnerability		Body size versus latent foraging		Phylogeny versus latent vulnerability		Phylogeny versus latent foraging	
Food web	Correlation coefficient	*P*	Correlation coefficient	*P*	Correlation coefficient	*P*	Correlation coefficient	*P*
1	.092	*.075*	.132	**.014**	.484	**<.001**	.660	**<.001**
2	.178	**.007**	.052	.143	−.043	.830	.222	**<.001**
3	.139	*.078*	.324	**<.001**	.224	**<.001**	−.018	.583
4	.124	*.052*	.409	**<.001**	.358	**<.001**	.399	**<.001**
5	.020	.340	.243	**<.001**	.75	**.037**	.289	**<.001**
6	.222	**<.001**	−.154	.974	−.094	.890	.153	**.001**
7	−.115	.974	.373	**<.001**	.012	.403	−.084	.967
8	.030	.285	.291	**<.001**	.225	**<.001**	.374	**<.001**
9	.221	*.089*	−.015	.522	.214	**.015**	−.095	.839
10	.000	.473	.168	**.002**	.042	.174	.076	**.019**
11	.033	.107	.021	.261	−.036	.700	.025	.338
12	.093	.116	−.181	.960	.005	.455	−.056	.790

Note: We compare body-size similarity with similarity of latent vulnerability and with latent foraging traits and phylogenetic similarity with similarity of latent vulnerability and with latent foraging traits. *P* values <.05 are indicated in bold; *P* values from .05 to .1 are indicated in italic type.

Conclusions

The body-size model is, to our knowledge, the first purely statistical model of food-web structure using an independent variable (body-size ratio) as a predictor of trophic interactions. We show how the inclusion of latent traits can dramatically improve the fit of the model and, more importantly, that these parameters can be used to shed light on the factors that structure trophic interactions in natural communities.

Our analyses reveal that the optimal body-size ratio does not capture all the trophic information of a food web and that the latent traits quantify a large part of the structure. First, the interpretation of latent traits shows that the effect of body size is not fully embodied in the optimal ratio, since for more than half of the food webs, body size is also correlated with the latent traits. More importantly, this additional effect of body size is found predominantly for the foraging traits. It might be speculated that this asymmetry is due to a more opportunistic behavior of predators, which pushes them to consume outside of the optimal body-size ecological range (Rossberg et al. 2006; Bersier and Kehrli 2008). Second, latent traits are related to phylogeny in most food webs, which confirms the importance of long-term evolution on community structure. However, the signal of phylogeny was not found in three webs for which latent traits nonetheless greatly improved the proportion of correctly predicted interactions. Without additional information on these systems, it is difficult to speculate on the biological factors that could account for this unexplained variation. The very value of latent traits is that they allow an exploration of such nontrivial structures.

Latent traits can also be used in meta-analyses to highlight general properties of systems. For example, we found that the increase of accuracy with the latent-trait model is more important for terrestrial webs (on average, by a factor of 7.8) than for aquatic webs (by an average factor of 4.5). This result indicates that the optimal ratio plays a larger role in aquatic environments than in terrestrial environments, which supports the finding that body size is a major driver of trophic interactions in the former systems (Shurin et al. 2006). Finally, latent traits as im-

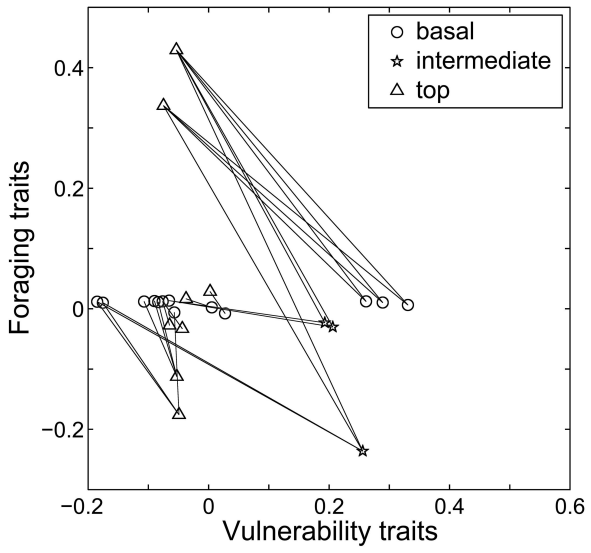

Figure 2: Estimated latent traits for the Goettingen food web. The lines indicate the trophic interactions.

plemented here (one trait assigned to outflows and one to inflows) could easily be applied to analyze networks in various domains of biology, from pollinators to protein networks.

Acknowledgments

We are indebted to S. Allesina, R. Naisbit, and an anonymous reviewer for their insightful comments on the manuscript. We thank J. Bascompte, O. Petchey, and A. Rossberg for their input and discussion. This work was supported by SystemsX.ch, the Swiss Initiative in Systems Biology (to L.-F.B. and C.M.), partly by the Swiss National Science Foundation (grant 3100A0-113843 to L.-F.B.), and partly by the National Centres of Competence in Research "Plant Survival" (to L.-F.B.).

Literature Cited

Allesina, S., D. Alonso, and M. Pascual. 2008. A general model for food web structure. Science 320:658–661.

Bersier, L.-F., and P. Kehrli. 2008. The signature of phylogenetic constraints on food-web structure. Ecological Complexity 5:132–139.

Bersier, L.-F., C. Banasek-Richter, and M. F. Cattin. 2002. Quantitative descriptors of food-web matrices. Ecology 83:2394–2407.

Brose, U., L. Cushing, E. L. Berlow, T. Jonsson, C. Banasek-Richter, L.-F. Bersier, J. L. Blanchard, et al. 2005. Body sizes of consumers and their resources. Ecology 86:2545.

Brose, U., T. Jonsson, E. L. Berlow, P. Warren, C. Banasek-Richter, L.-F. Bersier, J. L. Blanchard, et al. 2006. Consumer-resource body-size relationships in natural food webs. Ecology 87:2411–2417.

Cattin, M. F., L.-F. Bersier, C. Banasek-Richter, R. Baltensperger, and J. P. Gabriel. 2004. Phylogenetic constraints and adaptation explain food-web structure. Nature 427:835–839.

Cohen, J. E. 1977. Food webs and dimensionality of trophic niche space. Proceedings of the National Academy of Sciences of the USA 74:4533–4536.

Cohen, J. E., and C. M. Newman. 1985. A stochastic theory of community food webs. I. Models and aggregated data. Proceedings of the Royal Society B: Biological Sciences 224:421–448.

Cohen, J. E., F. Briand, and C. M. Newman. 1990. Community food webs: data and theory. Springer, Berlin.

Cohen, J. E., T. Jonsson, C. B. Muller, H. C. J. Godfray, and V. M. Savage. 2005. Body size of hosts and parasitoids in individual feeding relationships. Proceedings of the National Academy of Sciences of the USA 102:684–689.

Dawah, H. A., B. A. Hawkins, and M. F. Claridge. 1995. Structure of the parasitoid communities of grass-feeding chalcid wasps. Journal of Animal Ecology 64:708–720.

Drossel, B., P. G. Higgs, and A. J. McKane. 2001. The influence of predator-prey population dynamics on the long-term evolution of food web structure. Journal of Theoretical Biology 208:91–107.

Harper-Smith, S., E. L. Berlow, R. A. Knapp, R. J. Williams, and N. D. Martinez. 2005. Communicating ecology through food webs: visualizing and quantifying the effects of stocking alpine lakes with trout. Pages 407–423 *in* P. De Ruiter, J. C. Moor, and V. Wolters, eds. Dynamic food webs: multispecies assemblages, ecosystem development, and environmental change. Elsevier/Academic Press, London.

Hoff, P. D. 2009. Multiplicative latent factor models for description and prediction of social networks. Computational and Mathematical Organization Theory 15:261–272.

Jaccard, P. 1908. Nouvelles recherches sur la distribution florale. Bulletin de la Société Vaudoise des Sciences Naturelles 44:223–270.

Jonsson, T., J. E. Cohen, and S. R. Carpenter. 2005. Food webs, body size, and species abundance in ecological community description. Advances in Ecological Research 36:1–84.

Memmott, J., N. D. Martinez, and J. E. Cohen. 2000. Predators, parasitoids and pathogens: species richness, trophic generality and body sizes in a natural food web. Journal of Animal Ecology 69: 1–15.

Petchey, O. L., A. P. Beckerman, J. O. Riede, and P. H. Warren. 2008. Size, foraging, and food web structure. Proceedings of the National Academy of Sciences of the USA 105:4191–4196.

Pinnegar, J. K., V. M. Trenkel, A. N. Tidd, W. A. Dawson, and M. H. Du Buit. 2003. Does diet in Celtic Sea fishes reflect prey availability? Annual Symposium of the Fisheries Society of the British Isles 63:197–212.

Rossberg, A. G., H. Matsuda, T. Amemiya, and K. Itoh. 2006. Food webs: experts consuming families of experts. Journal of Theoretical Biology 241:552–563.

Shurin, J. B., D. S. Gruner, and H. Hillebrand. 2006. All wet or dried up? real differences between aquatic and terrestrial food webs. Proceedings of the Royal Society B: Biological Sciences 273:1–9.

Sokal, R., and F. J. Rohlf. 2001. Biometry. 3rd ed. Freeman, New York.

Sugihara, G., K. Schoenly, and A. Trombla. 1989. Scale-invariance in food web properties. Science 245:48–52.

Ulrich, W. 1999. Species composition, coexistence and mortality factors in a carrion exploiting community composed of necrophagous Diptera and their parasitoids (Hymenoptera). Polish Journal of Ecology 49:49–72.

Warren, P. H. 1989. Spatial and temporal variation in the structure of a fresh-water food web. Oikos 55:299–311.

Williams, R. J., and N. D. Martinez. 2000. Simple rules yield complex food webs. Nature 404:180–183.

Woodward, G., D. C. Speirs, and A. G. Hildrew. 2005. Quantification and resolution of a complex, size-structured food web. Advances in Ecological Research 36:85–135.

Associate Editor: Daniel L. Roelke
Editor: Mark A. McPeek

 DOI: 10.1086/653667

Appendix from R. P. Rohr et al., "Modeling Food Webs: Exploring Unexplained Structure Using Latent Traits"

(Am. Nat., vol. 176, no. 2, p. 170)

Supplementary Materials and Methods

Singular-Value Decomposition (SVD)

Let $\mathbf{M}$ be an $S \times S$ square matrix (we explain the SVD for square matrices, but it can be applied to any rectangular matrix). The singular value decomposition of $\mathbf{M}$ (see chap. 7 of Watkins 1991) is a factorization into a product of three matrices, $\mathbf{M} = \mathbf{VDF}$, where

$$\mathbf{V} = \begin{pmatrix} | & & | \\ \mathbf{v}^1 & \cdots & \mathbf{v}^S \\ | & & | \end{pmatrix},$$

$$\mathbf{D} = \begin{pmatrix} \delta_1 & & \\ & \ddots & \\ & & \delta_S \end{pmatrix},$$

$$\mathbf{F} = \begin{pmatrix} - & \mathbf{f}^1 & - \\ & \vdots & \\ - & \mathbf{f}^S & - \end{pmatrix}. \tag{A1}$$

The matrix $\mathbf{D}$ is a diagonal matrix with S nonnegative numbers $\delta_1, \ldots, \delta_S$ called the singular value of $\mathbf{M}$; $\mathbf{V}$ is a matrix of S orthogonal unitary (of length 1) column vectors $\mathbf{v}^1, \ldots, \mathbf{v}^S$; $\mathbf{F}$ is a matrix of S orthogonal unitary row vectors $\mathbf{f}^1, \ldots, \mathbf{f}^S$. Without loss of generality, is it always possible to reorder the singular values from the largest to the smallest, that is, $\delta_1 \geq \delta_2 \geq \ldots \geq \delta_S$; the columns of $\mathbf{V}$ and the rows of $\mathbf{F}$ must be reordered accordingly. Note that SVD is unique; that is, the singular values are unique up to their ordering, and the vectors are also unique up to their orientation in the space.

We can approximate the matrix $\mathbf{M}$ using the SVD in the following ways: The simplest approximation consists of considering only the first singular value (the largest) and setting all others to 0, that is, $\delta_2 = \ldots = \delta_S = 0$. This gives us $\mathbf{M} \approx \mathbf{v}^1\delta_1\mathbf{f}^1$, which corresponds exactly to the latent term in our latent-trait model. This approximation is called the first-rank approximation of $\mathbf{M}$.

The second-simplest approximation consists of considering only the two first singular values, which gives us $\mathbf{M} \approx \mathbf{v}^1\delta_1\mathbf{f}^1 + \mathbf{v}^2\delta_2\mathbf{f}^2$. This approximation is called the second-rank approximation of $\mathbf{M}$. We can continue until we consider all nonzero singular values; in the last case, we obtain exactly $\mathbf{M}$.

Note that SVD is closely related to principal component analysis. The singular values of the data matrix correspond to the eigenvalues of the covariance matrix. The columns of the matrix $\mathbf{V}$ are the eigenvectors of the covariance matrix.

Finally, note that the condition on the vectors $\mathbf{f}^i$ and $\mathbf{v}^i$ to be of unit length is not important for the computation of the similarity matrices (see "How to Relate Latent Traits to Biological Information"). Similarity matrices are independent of the choice of scale.

Estimation of the Parameters with Markov Chain Monte Carlo (MCMC) Techniques

To fit the parameters of the latent-trait model, maximum likelihood estimation could not be used because the likelihood function is too complex to maximize. Instead, we employed a Bayesian approach. Contrary to maximum likelihood, the parameters in the Bayesian framework are considered to be random variables. In this

context, we have to specify a prior distribution $p(\theta)$ for the parameter θ and determine the likelihood $p(y|\theta)$ of the model (y denotes the data). Using Bayes's theorem, we then obtain the posterior distribution of the parameters, that is, their distribution when the data are known:

$$p(\theta|y) = \frac{p(y|\theta)}{p(y)}p(\theta). \tag{A2}$$

These posterior distributions of the parameters are too complex to be computed analytically, and a common method is to "sample" these using an MCMC technique. The main idea is to take samples from a discrete-time Markov chain $(X_n)_{n\geq 0}$ whose stationary distribution is the posterior distribution of the parameters θ we are looking for and to let it run for a long time. Under certain not very restrictive conditions, the Markov chain will converge to its steady state and the X_n for large n can be considered as (certainly not independent) samples from the posterior distribution of the parameters. Moreover, it can be shown that

$$\frac{1}{N-k}\sum_{n=k}^{N} X_n \to E(\theta), \tag{A3}$$

as $N \to \infty$. In other words, the mean of the Markov chain will converge to the expected values of the parameters. Since this is true for any k, it can be useful to choose k such that the first and most imprecise values of the Markov chain (the so-called burn-in phase) are not taken into account. This will accelerate the convergence. For a good introduction to MCMC techniques and their application to Bayesian statistics, see Gilks et al. (1996) and Yang (2005). More precise and technical information can be found in Robert and Casella (2004).

Details of the Algorithm

The parameters to be estimated in the latent-trait model are α, β, γ, and δ and, for each species i (where $1 \leq i \leq S$), the latent traits $\mathbf{v}_i$ and $\mathbf{f}_i$. The data are the values (i.e., 0 or 1) of the food-web matrix $\mathbf{A}$. To construct the Markov chain in which stationary distribution converges to the posterior distribution of the parameters, we use the Metropolis-Hastings algorithm (sec. 3.4 of Yang 2005). In the next section, we describe the algorithm used. Finally we give some technical details concerning the distributions.

Metropolis-Hastings Algorithm

Algorithm: suppose the Markov chain to be constructed up to state n; more precisely, suppose α_n, β_n, γ_n, δ_n, $\mathbf{v}_n$, and $\mathbf{f}_n$ are known (note that $\mathbf{v}_n$ and $\mathbf{f}_n$ denote the vectors at the nth state of the Markov chain and not the nth components of the vectors).

Propose a new value α^* by sampling from $N(\alpha_n, \sigma_\alpha)$. Accept this new value and put $\alpha_{n+1} = \alpha^*$ with probability

$$\min\left\{1, \frac{p(\alpha^*|\beta_n, \gamma_n, \delta_n, \mathbf{v}_n, \mathbf{f}_n, \mathbf{A})}{p(\alpha_n|\beta_n, \gamma_n, \delta_n, \mathbf{v}_n, \mathbf{f}_n, \mathbf{A})}\right\}, \tag{A4}$$

else $\alpha_{n+1} = \alpha_n$.

Propose a new value β^* by sampling from $N(\beta_n, \sigma_\beta)$. Accept this new value and put $\beta_{n+1} = \beta^*$ with probability

$$\min\left\{1, \frac{p(\beta^*|\alpha_{n+1}, \gamma_n, \delta_n, \mathbf{v}_n, \mathbf{f}_n, \mathbf{A})}{p(\beta_n|\alpha_{n+1}, \gamma_n, \delta_n, \mathbf{v}_n, \mathbf{f}_n, \mathbf{A})}\right\}, \tag{A5}$$

else $\beta_{n+1} = \beta_n$.

Propose a new value γ^* by sampling from $N(\gamma_n, \sigma_\gamma)$. Accept this new value and put $\gamma_{n+1} = \gamma^*$ with probability

$$\min\left\{1, \frac{p(\gamma^*|\alpha_{n+1}, \beta_{n+1}, \delta_n, \mathbf{v}_n, \mathbf{f}_n, \mathbf{A})}{p(\gamma_n|\alpha_{n+1}, \beta_{n+1}, \delta_n, \mathbf{v}_n, \mathbf{f}_n, \mathbf{A})}\right\}, \tag{A6}$$

else $\gamma_{n+1} = \gamma_n$.

Propose a new value δ^* by sampling from $N(\delta_n, \sigma_\delta)$. Accept this new value and put $\delta_{n+1} = \delta^*$ with probability

$$\min\left\{1, \frac{p(\delta^*|\alpha_{n+1}, \beta_{n+1}, \gamma_{n+1}, \mathbf{v}_n, \mathbf{f}_n, \mathbf{A})}{p(\delta_n|\alpha_{n+1}, \beta_{n+1}, \gamma_{n+1}, \mathbf{v}_n, \mathbf{f}_n, \mathbf{A})}\right\}, \tag{A7}$$

else $\delta_{n+1} = \delta_n$.

Propose a new value $\mathbf{v}^*$ by sampling from vMF($\mathbf{v}_n$, $\boldsymbol{\kappa}_v$). Accept his new value and put $\mathbf{v}_{n+1} = \mathbf{v}^*$ with probability

$$\min\left\{1, \frac{p(\mathbf{v}^*|\alpha_{n+1}, \beta_{n+1}, \gamma_{n+1}, \delta_{n+1}, \mathbf{f}_n, \mathbf{A})}{p(\mathbf{v}_n|\alpha_{n+1}, \beta_{n+1}, \gamma_{n+1}, \delta_{n+1}, \mathbf{f}_n, \mathbf{A})}\right\}, \tag{A8}$$

else $\mathbf{v}_{n+1} = \mathbf{v}_n$.

Propose a new value $\mathbf{f}^*$ by sampling from vMF($\mathbf{f}_n$, $\boldsymbol{\kappa}_f$). Accept his new value and put $\mathbf{f}_{n+1} = \mathbf{f}^*$ with probability

$$\min\left\{1, \frac{p(\mathbf{f}^*|\alpha_{n+1}, \beta_{n+1}, \gamma_{n+1}, \delta_{n+1}, \mathbf{v}_{n+1}, \mathbf{A})}{p(\mathbf{f}_n|\alpha_{n+1}, \beta_{n+1}, \gamma_{n+1}, \delta_{n+1}, \mathbf{v}_{n+1}, \mathbf{A})}\right\}, \tag{A9}$$

else $\mathbf{f}_{n+1} = \mathbf{f}_n$. Here vMF($\mu$, κ) denotes the von Mises-Fisher distribution, which is a distribution on the unit sphere in $\mathbf{R}^S$, parameterized by its mean direction μ and concentration parameter κ. The sampling technique for a von Mises-Fisher distribution is explained in Wood (1994).

Likelihood, Prior and Posterior Distribution

The prior distributions of the parameters α, β, γ, δ, $\mathbf{v}$, and $\mathbf{f}$ are chosen to be independent and of the following types: normal for α, β, γ, and δ and uniform on the unit sphere in $\mathbf{R}^S$ for $\mathbf{v}$ and $\mathbf{f}$ (recall once again that $\mathbf{v}$ and $\mathbf{f}$ are of length 1). As explained in the preceding section, it is necessary to compute the acceptance probabilities for the proposal values of the parameters. These probabilities are expressed as quotients of posterior probabilities of the parameters. As an illustration of how these probabilities can be simplified, consider the case of the parameter α: since the prior distributions of the parameters α, β, γ, δ, $\mathbf{v}$, and $\mathbf{f}$ are assumed to be independent, Bayes's theorem yields

$$p(\alpha^*|\beta, \gamma, \delta, \mathbf{v}, \mathbf{f}, \mathbf{A}) = \frac{p(\mathbf{A}|\alpha^*, \beta, \gamma, \delta, \mathbf{v}, \mathbf{f})}{p(\beta, \gamma, \delta, \mathbf{v}, \mathbf{f}, \mathbf{A})} p(\alpha^*),$$

$$p(\alpha_n|\beta, \gamma, \delta, \mathbf{v}, \mathbf{f}, \mathbf{A}) = \frac{p(\mathbf{A}|\alpha_n, \beta, \gamma, \delta, \mathbf{v}, \mathbf{f})}{p(\beta, \gamma, \delta, \mathbf{v}, \mathbf{f}, \mathbf{A})} p(\alpha_n).$$

Hence, the only function needed to compute the acceptance probabilities are the likelihood function and the prior distribution, which are both known:

$$\frac{p(\alpha^*|\beta, \gamma, \delta, \mathbf{v}, \mathbf{f}, \mathbf{A})}{p(\alpha_n|\beta, \gamma, \delta, \mathbf{v}, \mathbf{f}, \mathbf{A})} = \frac{p(\mathbf{A}|\alpha^*, \beta, \gamma, \delta, \mathbf{v}, \mathbf{f}) p(\alpha^*)}{p(\mathbf{A}|\alpha_n, \beta, \gamma, \delta, \mathbf{v}, \mathbf{f}) p(\alpha_n)}.$$

By definition of the model, the likelihood function is

$$p(\mathbf{A}|\alpha, \beta, \gamma, \delta, \mathbf{v}, \mathbf{f}) = \prod_{i,j=1}^{S} \Pr(a_{ij} = 1)^{a_{ij}} \Pr(a_{ij} = 0)^{1-a_{ij}},$$

where $\Pr(a_{ij} = 1) = e^{\theta_{ij}}/(1 + e^{\theta_{ij}})$ for $\theta_{ij} = \log[\Pr(a_{ij} = 1)/\Pr(a_{ij} = 0)]$, the logit of the linking probability, is given by the equation of the latent-trait model (see "Latent-Trait Model").

Literature Cited Only in the Appendix

Gilks, W. R., S. Richardson, and D. J. Spiegelhalter. 1996. Markov chain Monte Carlo in practice. Chapman & Hall, London.

Robert, C. P., and G. Casella. 2004. Monte Carlo statistical methods. 2nd ed. Springer, New York.

Watkins, D. S. 1991. Fundamentals of matrix computations. Wiley, New York.

Wood, A. T. A. 1994. Simulation of the von Mises Fisher distribution. Communications in Statistics 23:157–164.

Yang, Z. 2005. Bayesian inference in molecular phylogenetics. Pages 63–90 *in* O. Gascuel, ed. Mathematics of evolution and phylogeny. Oxford University Press, Oxford.

Table A1: Descriptions of the 12 studied food webs

N	Common name	Geographic location	General habitat	Specific habitat	pw/fw *
1	Silwood Park	United Kingdom; UTM: 51.24'N, 0.34'W; Silwood Park, Berkshire	terrestrial	abandoned field	pw
2	Grassland	United Kingdom	terrestrial	grasslands	fw
3	Sierra Lakes	United States of America; John Muir Wilderness Area and Kings Canyon National Park, Sierra Nevada mountains, California	freshwater	small subalpine and alpine lakes, less than 3m deep	fw
4	Tuesday Lakes	United States of America; UTM: 89.32'W, 46.13'N; Tuesday Lake, Michigan	freshwater	small, mildly acidic lake, 1984	fw
5	Mill Stream	United Kingdom; the River Frome, Dorset; UTM: 50.40'N, 2.11'W	freshwater	lowland chalk stream	fw
6	Broom	United Kingdom; UTM: 51.24'N, 0.34'W; Silwood Park, Berkshire	terrestrial	*Cytisis scoparius* (Scotch broom) patch, source web on broom	fw
7	Celtic Sea	Europe, Celtic Sea ecosystem	marine	demersal food web	pw
8	Mulgrave River	Australia; Mulgrave River; UTM: 17.08'S, 145.52'E	freshwater	lowland coastal river	pw
9	Goettingen	Germany; Goettingen; UTM: 51.31'N, 09.56'E;	terrestrial	Beech forest	pw
10	Skipwith Pond	United Kingdom; UTM: 53.40'N, 0.59'W; Skipwith Common, North Yorkshire	freshwater	acidic pond, up to 1 m deep, 0.25 ha	fw
11	Sheffield	United Kingdom; Sheffield;	freshwater	laboratory study	pw
12	Broadstone Stream	United Kingdom; UTM: 51.05'N, 0.03'E; Broadstone Stream in Sussex	freshwater	spring-fed acidic headwater stream, 120m elevation	fw

*fw indicates a complete food web, pw a partial web

Table A2: Results of the Mantel tests comparing the similarity in latent traits of vulnerability (foraging) with the Jaccard index of vulnerability (foraging).

	Vul. traits vs. Jaccard vul.		For. traits vs. Jaccard for.	
Food web	corr. coeff.	p-value	corr. coeff.	p-value for
1	0.502	<**0.001**	0.196	**0.004**
2	0.304	<**0.001**	0.042	0.183
3	0.540	<**0.001**	0.061	0.224
4	0.669	<**0.001**	0.424	<**0.001**
5	0.227	<**0.001**	0.596	<**0.001**
6	-0.006	0.525	0.465	<**0.001**
7	0.273	<**0.001**	0.352	<**0.001**
8	0.397	<**0.001**	0.224	<**0.001**
9	0.404	<**0.001**	0.193	<**0.001**
10	0.320	<**0.001**	0.280	<**0.001**
11	0.379	<**0.001**	0.465	<**0.001**
12	0.286	**0.008**	0.419	<**0.001**

Boldface type indicates p-values ≤ 0.01.

For each of the 12 studied food webs, there are three pages.

1st page. This figure is the same as Fig. 1 in the main article: comparison of the Body Size Model and the Latent Trait Model. Figures a and d show, with respect to log body size ratio, the coefficients of the observed predation matrix in blue and the fitted linking probabilities in red (note that these are individual points corresponding to all possible pairs of species). The black curve illustrates the part of the fitted linking probability contributed by the body size term of the corresponding model. The dashed line indicates the threshold above which the fitted linking probabilities are interpreted as trophic links. Figures b and e show the observed predation matrix, where black circles represent trophic links. The background color illustrates the magnitudes of the corresponding predicted linking probabilities, increasing from pale yellow to red. Figures c and f show again the magnitudes of the fitted linking probabilities, now overlaid with the fitted predation matrix.

2nd page. Upper figure : graph of the estimated foraging against the estimated vulnerability traits Symbols indicate trophic level and lines represent trophic interactions. Lower left and right : 3-dimensional graph of the number of consumers and number of resources, respectively, against. the estimated latent traits.

3nd page. Names of the species in the food web. The numbering is the same as in the preceding graphs.

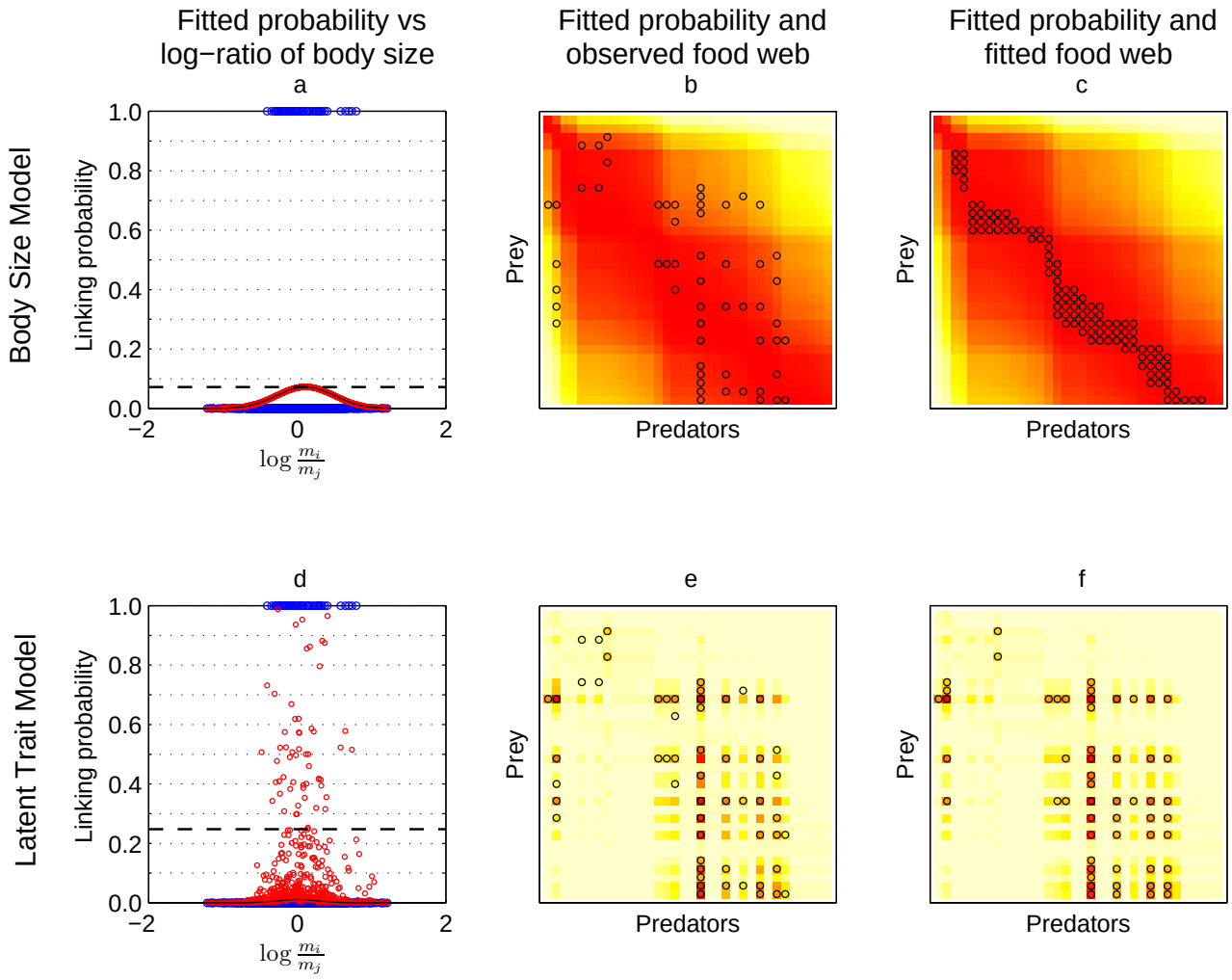

Figure A1: Silwood Park

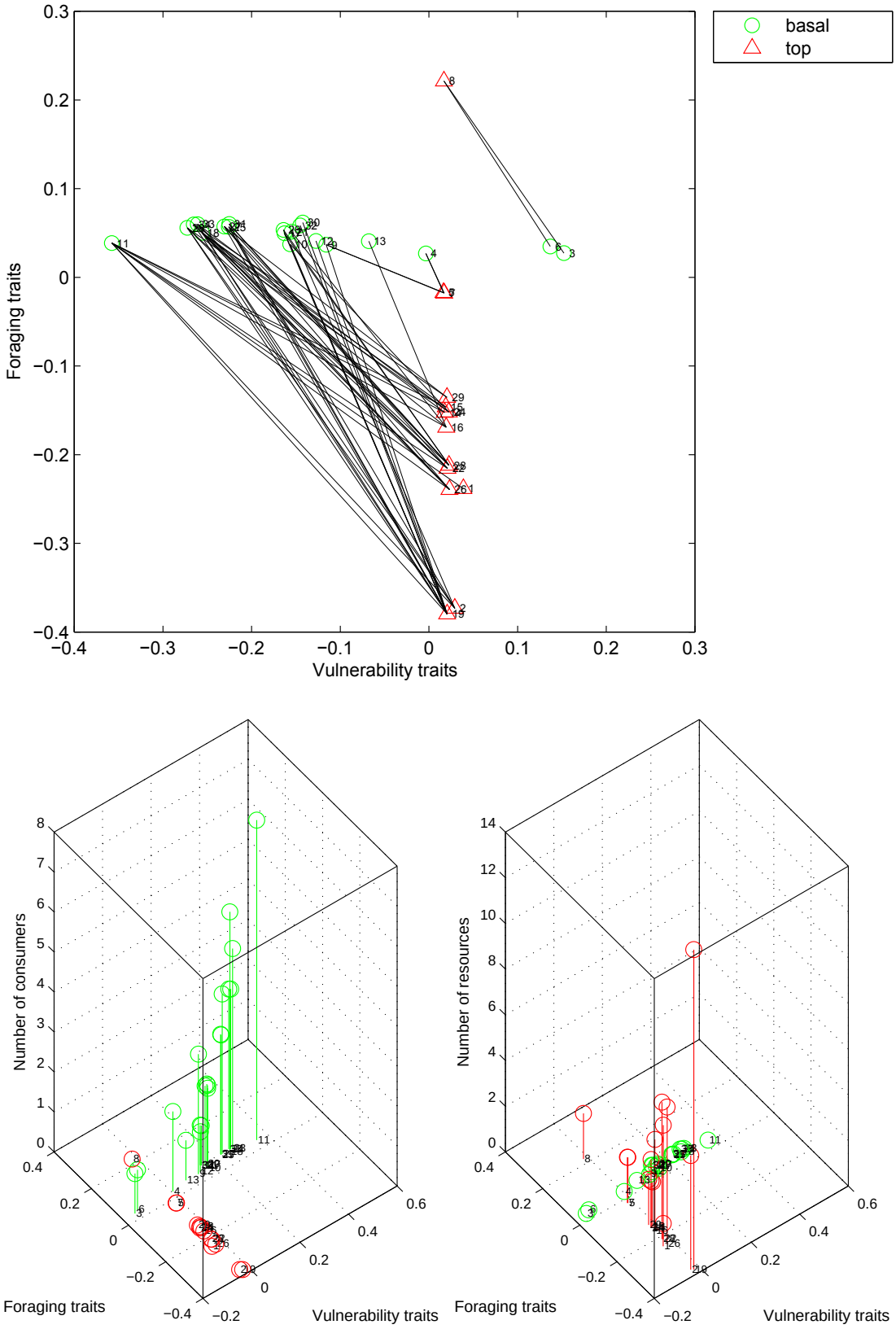

Figure A2: Silwood Park

Silwood Park	
Sp. no.	Species name
1	Aphelinus varipes adults
2	Aphelinus abdominalis adults
3	Capitophorus carduinis larvae
4	Aphis larvae
5	Binodoxys acalephe adults
6	Capitophorus carduinis adults
7	Praon abjectum adults
8	Aphidius matricariae adults
9	Aphis adults
10	Megoura viciae larvae
11	Sitobion larvae
12	Sitobion ptericolens larvae
13	Metopolophium albidum larvae
14	Praon volucre adults
15	Ephedrus plagiator adults
16	Aphidius rhopalosiphi adults
17	Amphorophora rubi larvae
18	Sitobion adults
19	Praon dorsale adults
20	Macrosiphum funestum larvae
21	Metopolophium albidum adults
22	Aphidius ervi adults
23	Acyrthosiphon pisum larvae
24	Aphidius eadyi adults
25	Amphorophora rubi adults
26	Aphidius picipes adults
27	Microlophium carnosum larvae
28	Aphidius urticae adults
29	Aphidius microlophii adults
30	Sitobion ptericolens adults
31	Macrosiphum funestum adults
32	Megoura viciae adults
33	Acyrthosiphon pisum adults
34	Microlophium carnosum adults

Table A3

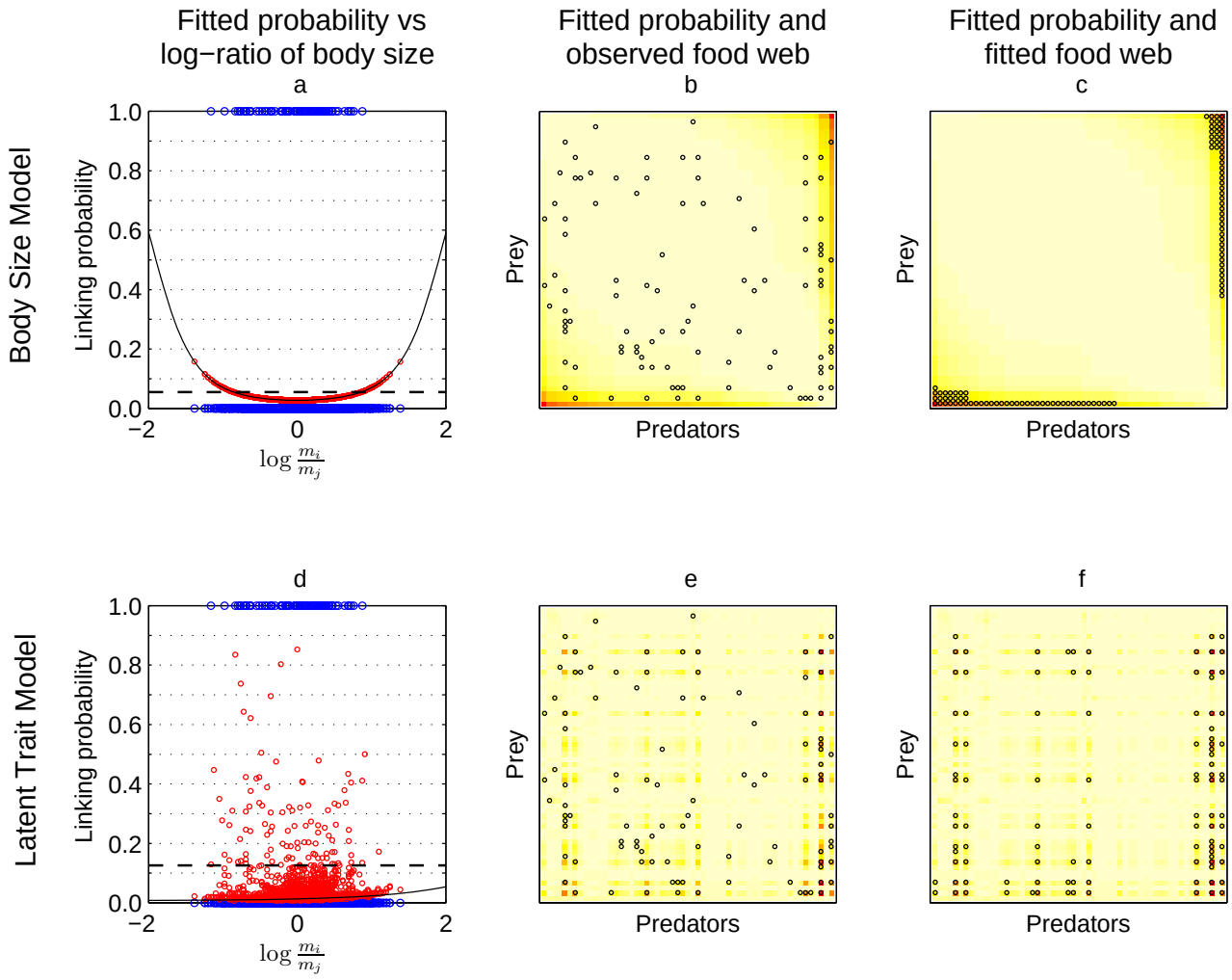

Figure A3: Grassland

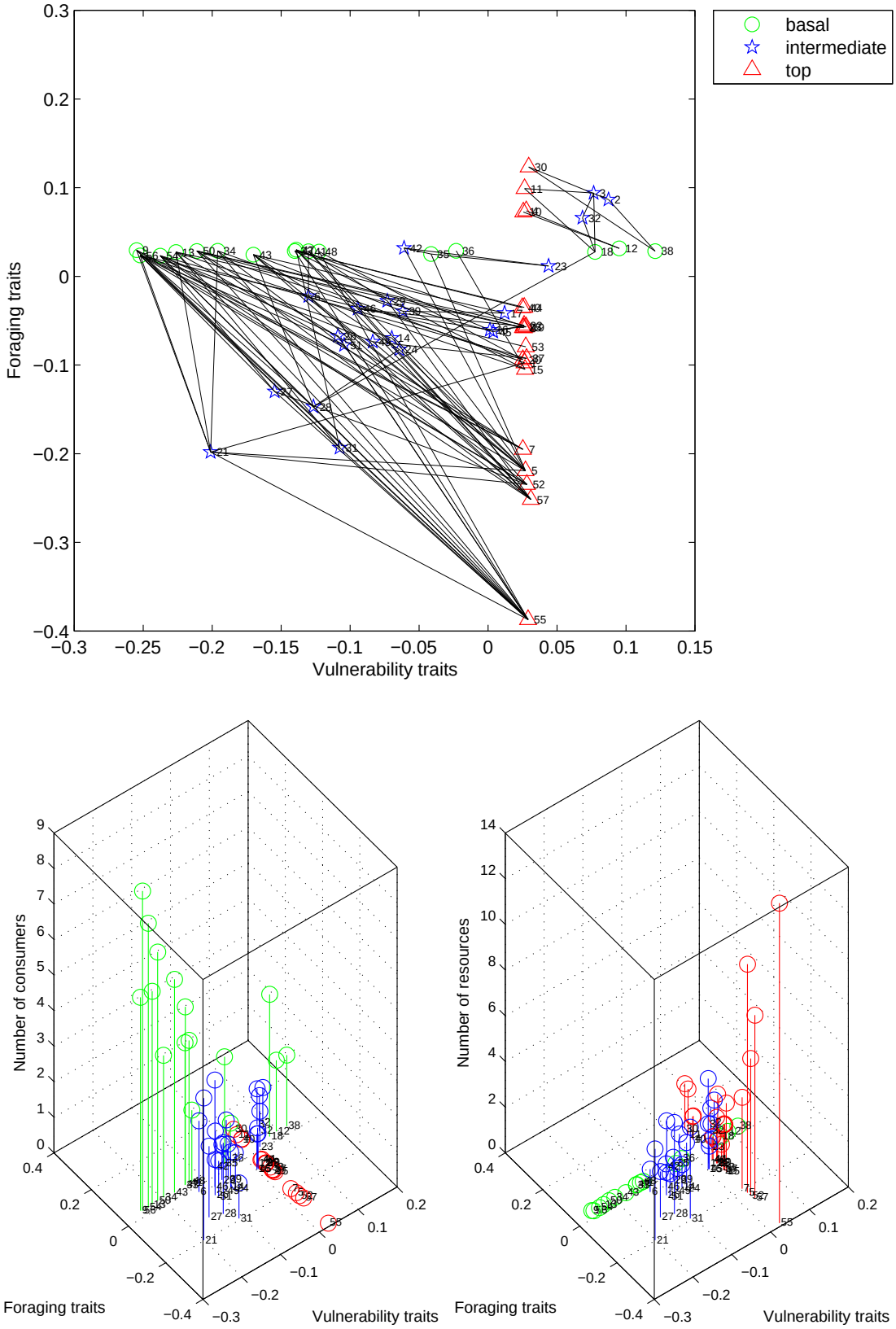

Figure A4: Grassland

Grassland			
Sp. no.	Species name	Sp. no.	Species name
1	Pediobius festucae larvae	41	Tetramesa hyalipennis larvae
2	Pediobius claridgei larvae	42	Pediobius dactylicola larvae
3	Pediobius planiventris larvae	43	Tetramesa longicornis larvae
4	Pediobius alaspharus larvae	44	Chlorocytus larvae
5	Mesopolobus graminum larvae	45	Eurytoma tapio larvae
6	Eurytoma roseni larvae	46	Eurytoma appendigaster larvae
7	Sycophila mellea larvae	47	Tetramesa petiolata larvae
8	Eurytoma flavimana larvae	48	Ahtola atra larvae
9	Tetramesa brevicornis larvae	49	Eurytoma pollux larvae
10	Chlorocytus agropyri larvae	50	Tetramesa angustipennis larvae
11	Chlorocytus formosus larvae	51	Chlorocytus harmolitae larvae
12	Tetramesa cornuta larvae	52	Eupelmus atropurpureus larvae
13	Tetramesa linearis larvae	53	Eurytoma danuvica larvae
14	Homoporus fulviventris larvae	54	Tetramesa calamagrostis larvae
15	Pediobius larvae	55	Macroneura vesicularis larvae
16	Pediobius deschampiae larvae	56	Tetramesa eximia larvae
17	Eurytoma phalaridis larvae	57	Endromopoda larvae
18	Tetramesa fulvicollis larvae		
19	Chlorocytus deschampiae larvae		
20	Chlorocytus pulchripes larvae		
21	Eurytoma larvae		
22	Pediobius eubius larvae		
23	Eurytoma erdoesi larvae		
24	Chlorocytus phalaridis larvae		
25	Homoporus febriculosus larvae		
26	Homoporus luniger larvae		
27	Torymus baudysi larvae		
28	Bracon larvae		
29	Bracon erythrostictus larvae		
30	Chlorocytus ulticonus larvae		
31	Homoporus larvae		
32	Eurytoma collaris larvae		
33	Tetramesa airae larvae		
34	Tetramesa brevicollis larvae		
35	Tetramesa longula larvae		
36	Tetramesa albomaculata larvae		
37	Pediobius calamagrostidis larvae		
38	Tetramesa phleicola larvae		
39	Pediobius phalaridis larvae		
40	Eurytoma castor larvae		

Table A4

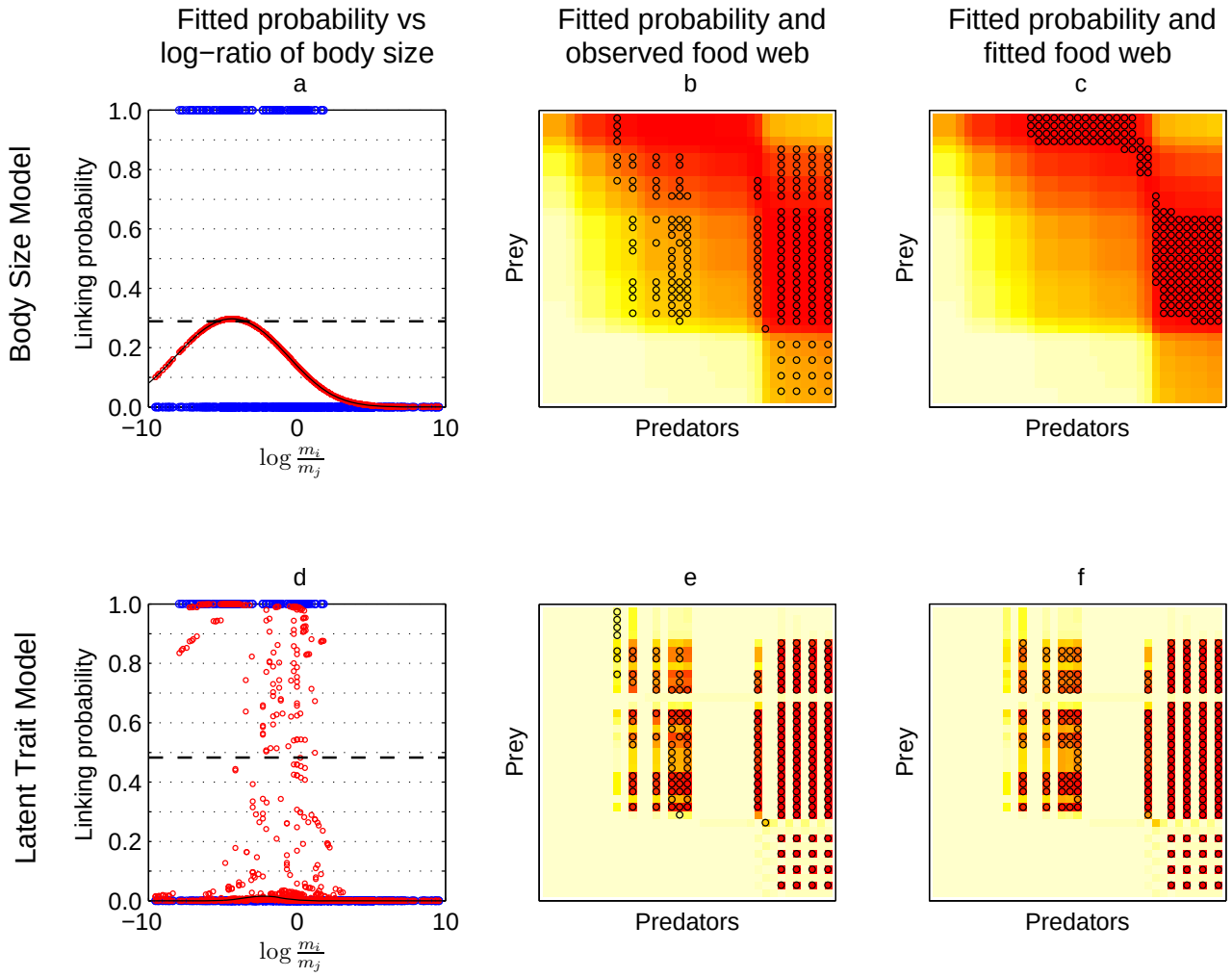

Figure A5: Sierra Lakes

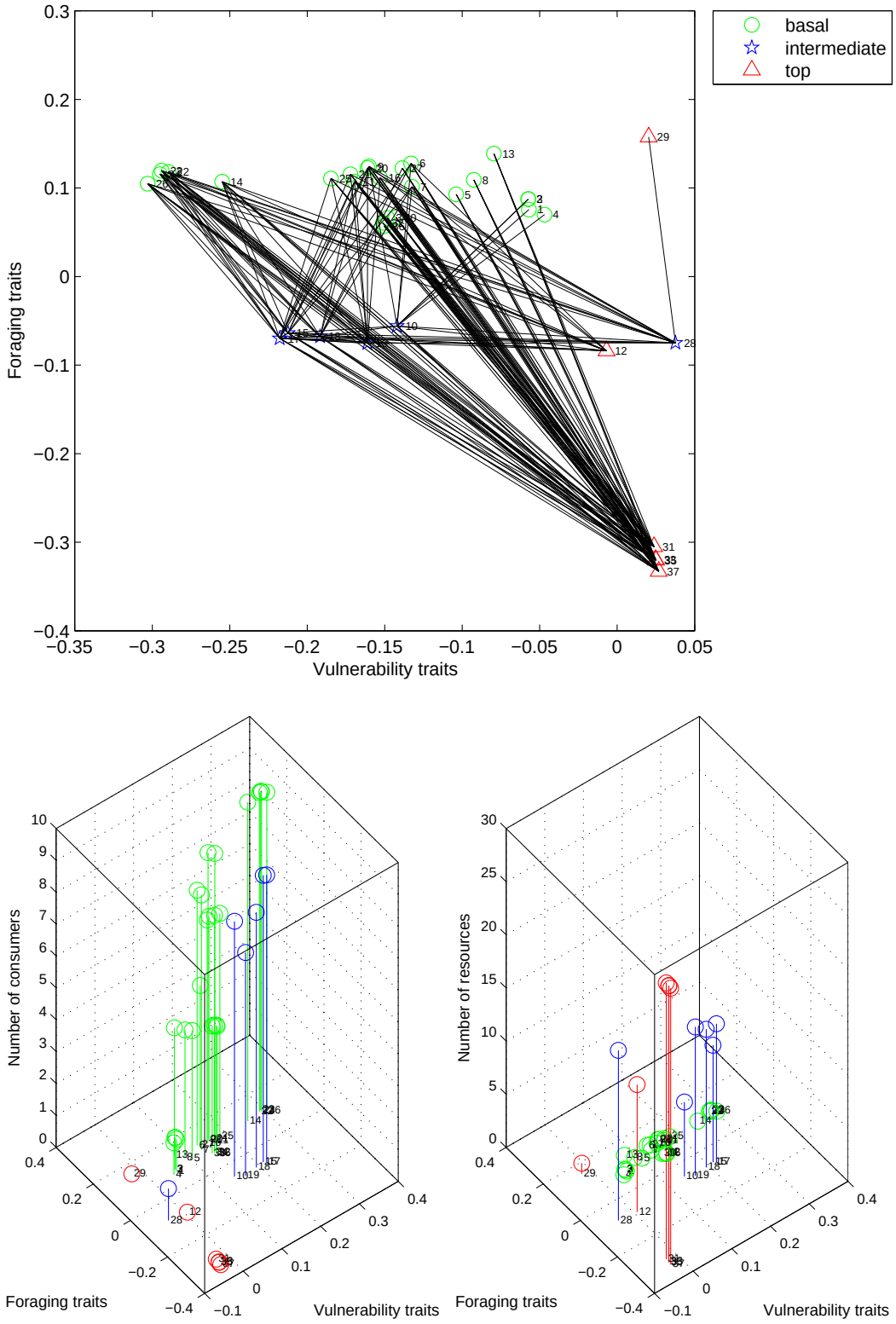

Figure A6: Sierra Lakes

Sierra Lakes	
Sp. no.	Species name
1	Keratella
2	Keratella quadrata
3	Polyarthra
4	Kellicottia
5	Chydorus sphaericus
6	Daphnia rosea
7	Leptodiaptomus signicauda
8	Cyclopoda
9	Daphnia middendorffiana
10	Hesperodiaptomus shoshone
11	Hydroporini adults
12	Hydroporini larvae; adults
13	Pisidium
14	Culex
15	Corixidae
16	Psychoglypha
17	Sialis
18	Agabus
19	Polycentropus
20	Limnephilus
21	Desmona
22	Callibaetis ferrugineus
23	Chironomidae
24	Ameletus
25	Hesperophylax
26	Oligochaeta
27	Rana muscosa larvae
28	Rana muscosa adults
29	Thamnophis elegans elegans
30	Salvelinus fontinalis
31	Salvelinus fontinalis adults
32	Oncorhynchus mykiss aguabonita
33	Oncorhynchus mykiss aguabonita adults
34	Oncorhynchus mykiss
35	Oncorhynchus mykiss adults
36	Salmo trutta
37	Salmo trutta adults

Table A5

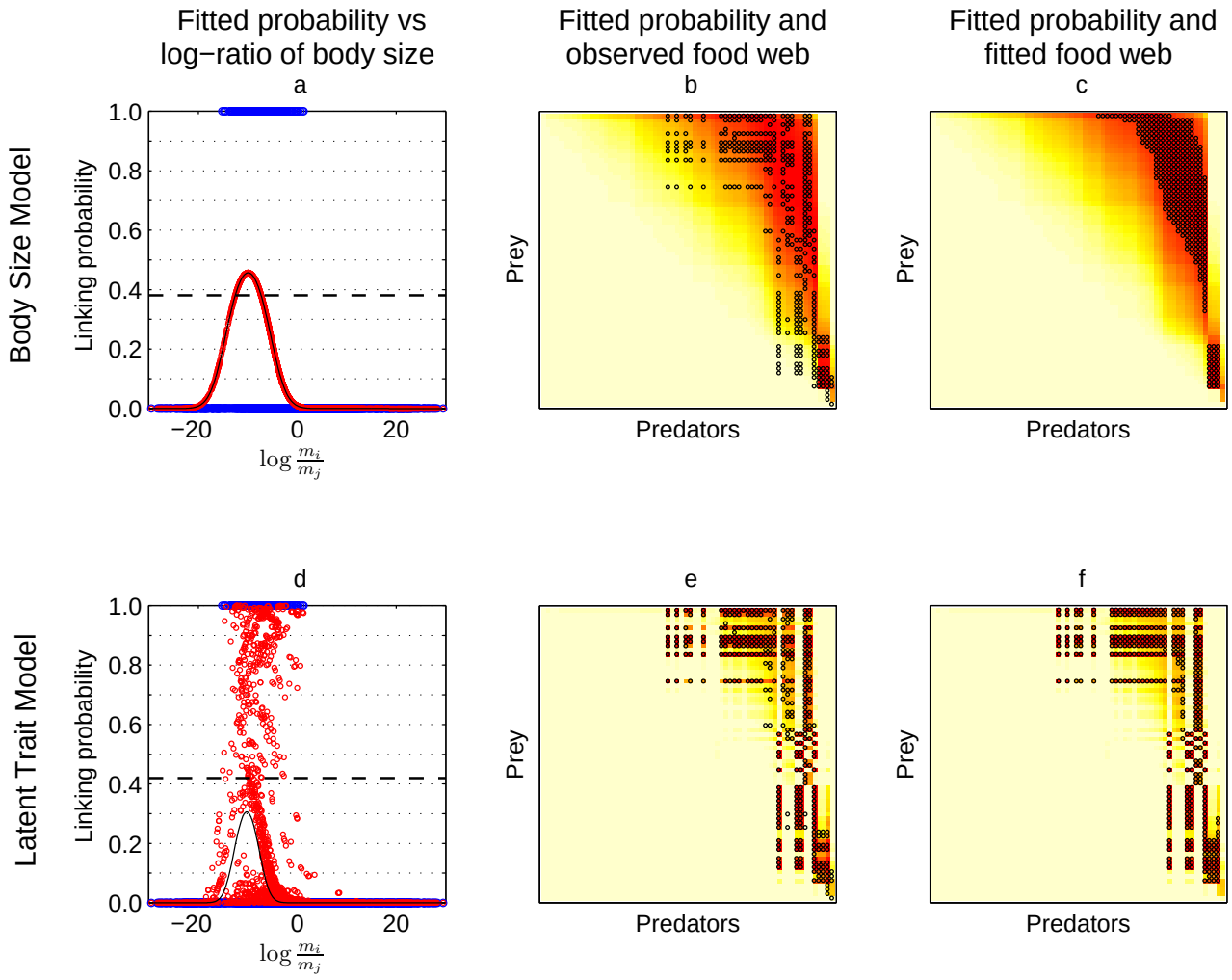

Figure A7: Tuesday Lake

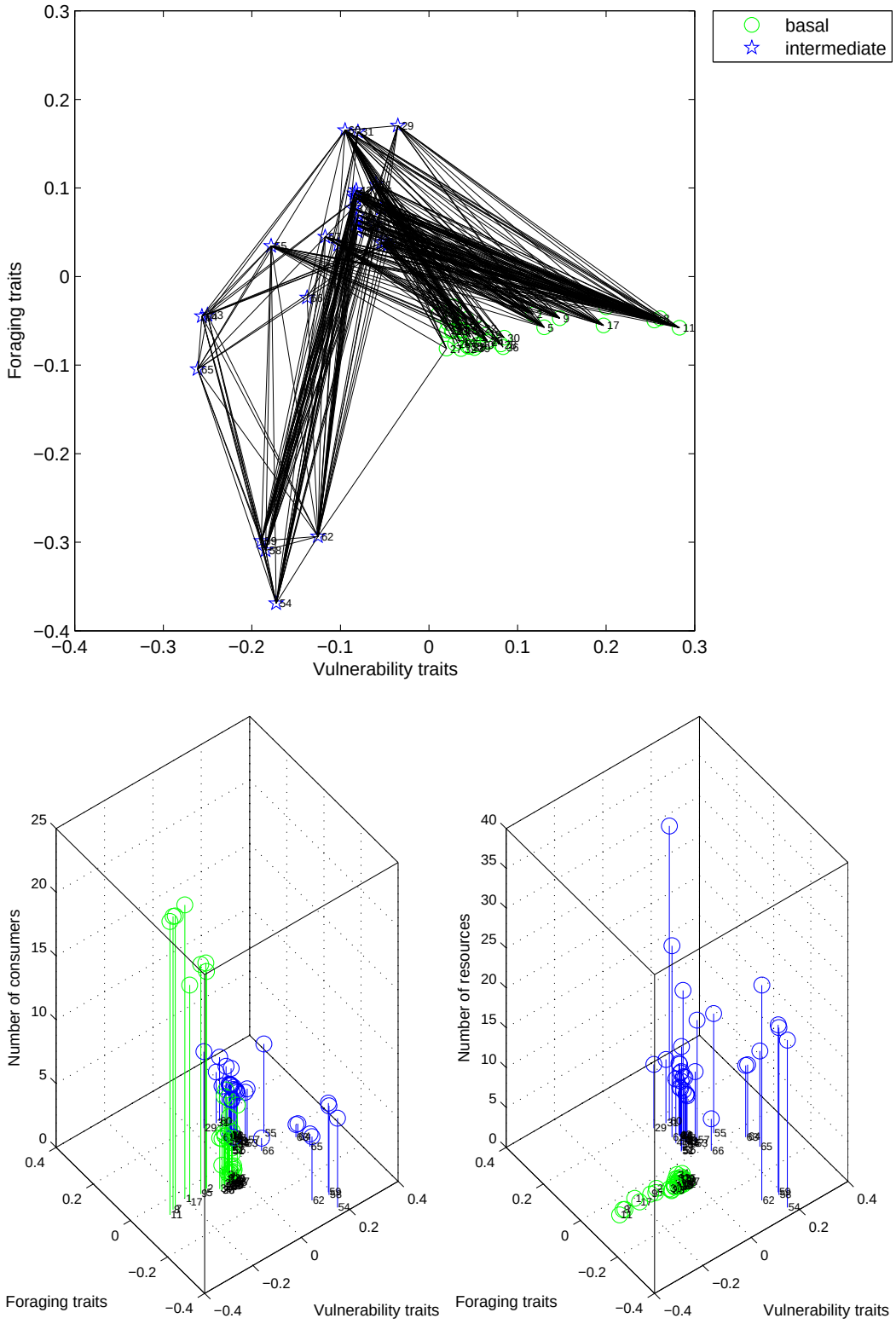

Figure A8: Tuesday Lake

Tuesday Lake			
Sp. no.	Species name	Sp. no.	Species name
1	Chromulina	41	Ploesoma
2	Unclassified microflagellates	42	Gastropus stylifer
3	Ankistrodesmus spiralis	43	Gastropus hyptopus
4	Ankyra judai	44	Conochiloides dossuarius
5	Trachelomonas	45	Trichocerca multicrinis
6	Closteriopsis longissima	46	Filinia longispina
7	Chroococcus dispersus	47	Ascomorpha eucadis
8	Selenastrum minutum	48	Polyarthra vulgaris
9	Unclassified flagellates	49	Trichocerca cylindrica
10	Dictyosphaerium pulchellum	50	Synchaeta
11	Cryptomonas	51	Bosmina longirostris
12	Schroederia setigera	52	Diaphanosoma leuchtenbergianum
13	Dinobryon sociale	53	Conochilus
14	Nostoc	54	Tropocyclops prasinus
15	Quadrigula	55	Leptodiaptomus siciloides
16	Mallomonas	56	Daphnia rosea
17	Chroococcus limneticus	57	Skistodiaptomus oregonensis
18	Arthrodesmus	58	Cyclops varicans rubellus
19	Peridinium pusillum	59	Orthocyclops modestus
20	Oscillatoria	60	Daphnia pulex
21	Dinobryon cylindricum	61	Holopedium gibberum
22	Cosmarium	62	Chaoborus punctipennis
23	Dinobryon bavaricum	63	Phoxinus eos
24	Oocystis	64	Phoxinus neogaeus
25	Glenodinium pulvisulcus	65	Umbra limi
26	Quadrigula lacustris	66	Micropterus salmoides
27	Glenodinium quadridens		
28	Dinobryon sertularia		
29	Keratella cochlearis		
30	Sphaerocystis schroeteri		
31	Keratella testudo		
32	Microcystis aeruginosa		
33	Kellicottia		
34	Kellicottia bostoniensis		
35	Peridinium wisconsinense		
36	Peridinium cinctum		
37	Kellicottia longispina		
38	Synedra		
39	Peridinium limbatum		
40	Gloeocystis		

Table A6

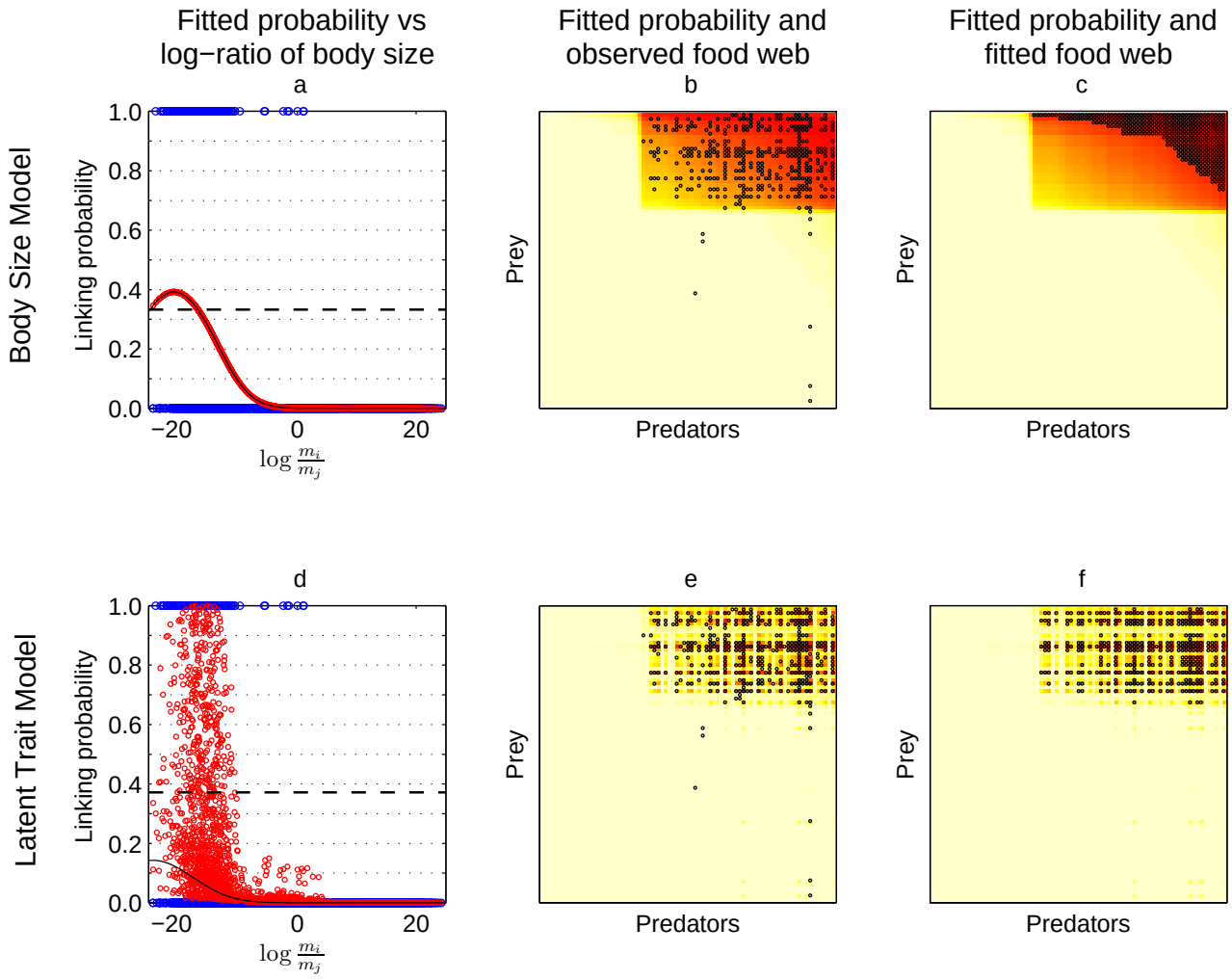

Figure A9: Mill Stream

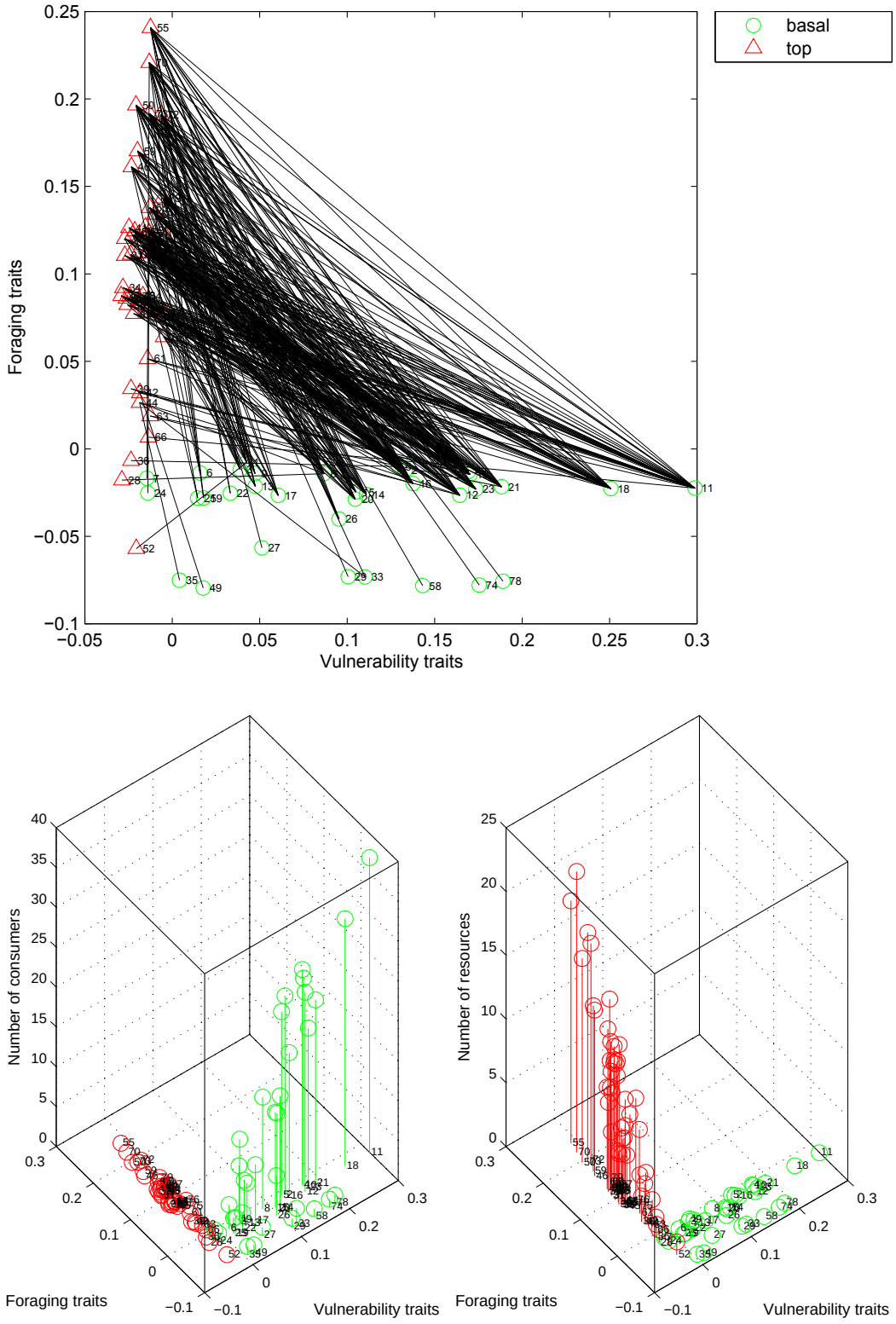

Figure A10: Mill Stream

Mill Stream			
Sp. no.	Species name	Sp. no.	Species name
1	Cyanobacteria	41	Pericoma trivialis larvae
2	Fragilaria elliptica	42	Procladius larvae
3	Achnanthes elliptica	43	Pisidium adults; juveniles
4	Gomphonema olivaceum	44	Macropelopia larvae
5	Amphora pediculus	45	Limnophila larvae
6	Fragilaria leptostauron	46	Limonia larvae
7	Achnanthes lanceolata	47	Antocha vitripennis larvae
8	Gongrosira incrustans	48	Tinodes waeneri larvae
9	Cymbella minuta	49	Microtendipes
10	Melosira varians	50	Microtendipes larvae
11	Cocconeis placentula	51	Athripsodes cinereus larvae
12	Navicula menisculus	52	Aphelocheirus aestivalis larvae
13	Surirella ovalis	53	Lumbriculidae adults; juveniles
14	Navicula gregaria	54	Eiseniella tetraedra adults; juveniles
15	Nitzschia dissipata	55	Valvata piscinalis adults; juveniles
16	Nitzschia perminuta	56	Polycentropus flavomaculatus larvae
17	Fragilaria vaucheriae	57	Gammarus pulex adults; juveniles
18	Rhoicosphenia curvata	58	Simuliidae
19	Ostracoda	59	Simuliidae larvae
20	Diatoma vulgare	60	Asellus aquaticus adults; juveniles
21	Navicula tripunctata	61	Limnophora larvae
22	Amphora ovalis	62	Potamopyrgus jenkinsi adults; juveniles
23	Navicula lanceolata	63	Limnius larvae
24	Gyrosigma obtusatum	64	Theodoxus fluviatilis adults; juveniles
25	Ciliophora	65	Anabolia nervosa larvae
26	Cymatopleura solea	66	Brychius elevatus larvae
27	Nematoda	67	Potamophylax latipennis larvae
28	Synorthocladius larvae	68	Hydropsyche larvae
29	Cricotopus	69	Halesus radiatus larvae
30	Cricotopus larvae	70	Lymnea peregra adults; juveniles
31	Hydroptila larvae	71	Ancylus fluviatilis adults; juveniles
32	Naididae adults; juveniles	72	Brachycentrus subnubilus larvae
33	Heterotrissocladius	73	Erpobdella octoculata adults; juveniles
34	Heterotrissocladius larvae	74	Ephemera danica
35	Pentaneura	75	Ephemera danica larvae
36	Rhyacophila dorsalis larvae	76	Sialis lutaria larvae
37	Limnephilus larvae	77	Sericostoma personatum larvae
38	Elmis aenea larvae	78	Tipula montium
39	Bezzia larvae	79	Tipula montium larvae
40	Tubificidae adults; juveniles		

Table A7

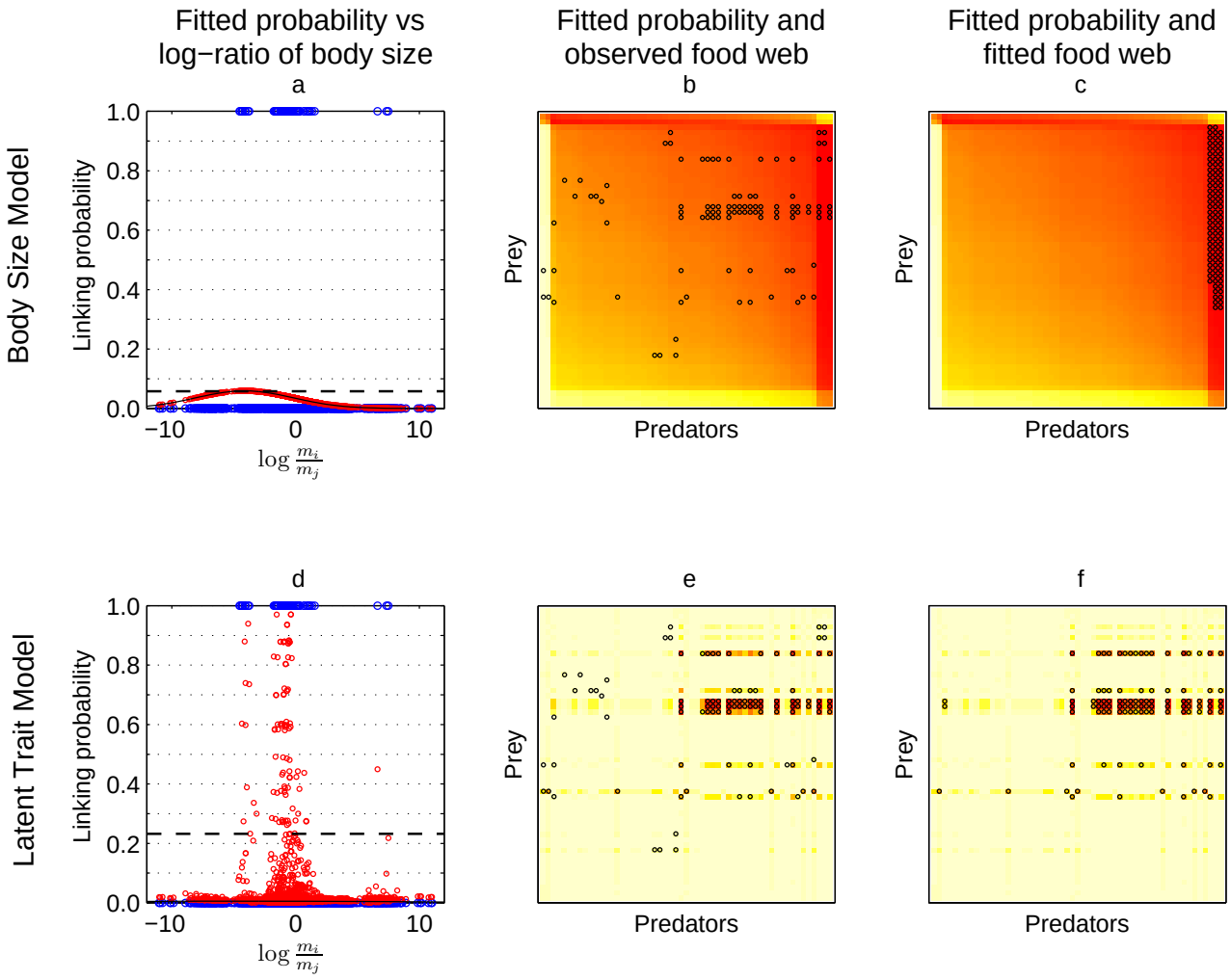

Figure A11: Broom

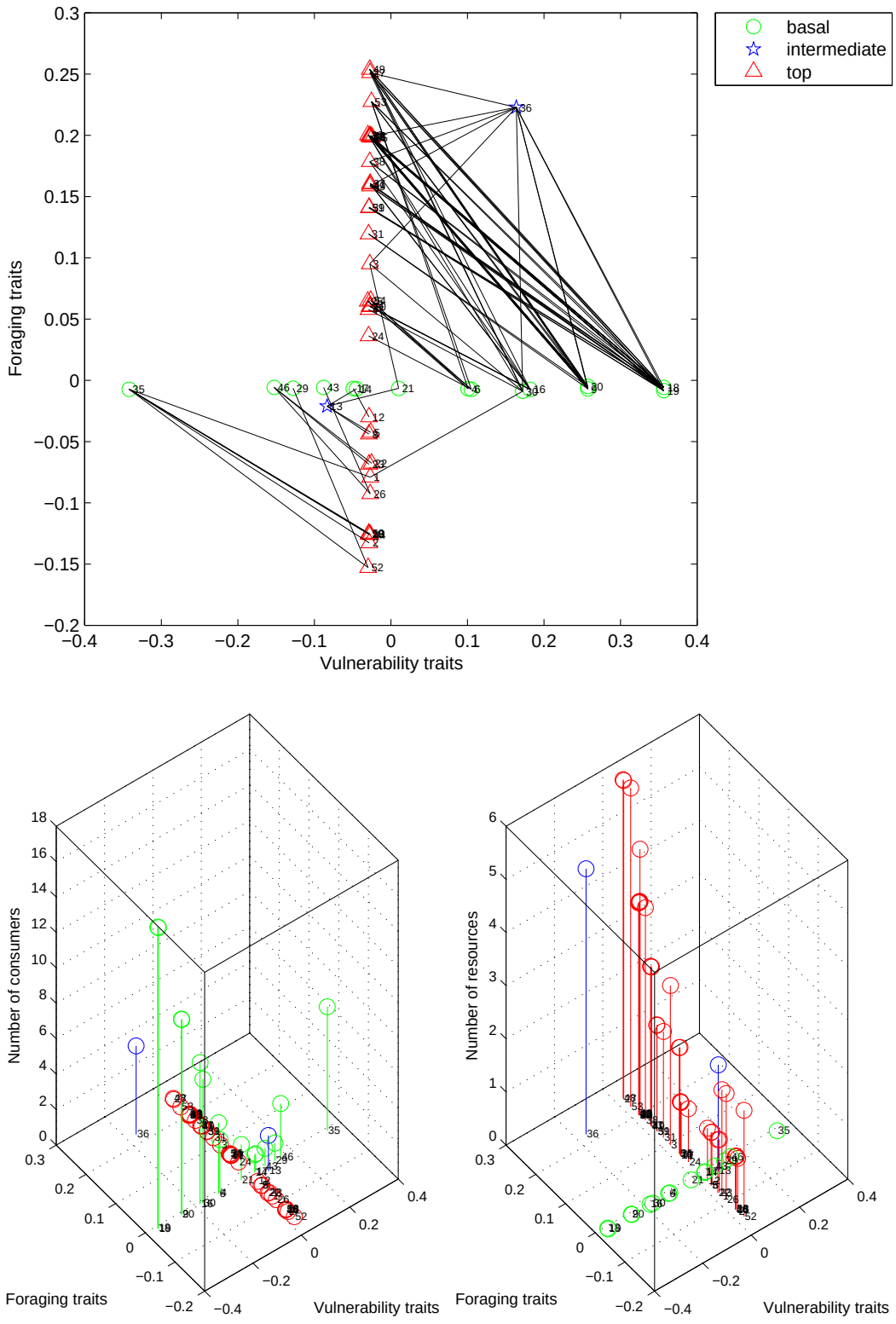

Figure A12: Broom

Broom			
Sp. no.	Species name	Sp. no.	Species name
1	Beauveria bassiana	41	Meta segmentata
2	Paecilomyces	42	Coccinella septempunctata
3	Anystis baccarum	43	Agonopteryx assimilella
4	Hylastinus obscurus	44	Xantholinus linearis
5	Mesopolobus mediterraneus	45	Anatis ocellata
6	Phloeophthorus rhododactylus	46	Chesias legatella
7	Necremnus metalarus	47	Harpalus rubripes
8	Aprostocetus tibialis	48	Forficula auricularia
9	Acyrthosiphon spartii	49	Araneus diadematus
10	Chrysocharis gemma	50	Philonthus politus
11	Pringalio soemias	51	Pisaura mirabilis
12	Microctonus	52	Abax parallelepipedus
13	Habrocytus sequester	53	Parus caeruleus
14	Apion fuscirostre	54	Parus major
15	Centistes excrucians	55	Fringilla coelebs
16	Leucoptera spartifoliella		
17	Apion immune		
18	Arytaina genistae		
19	Arytaina spartii		
20	Aphis sarathamni		
21	Bruchidius ater		
22	Apanteles fulvipes		
23	Apanteles vitripennis		
24	Cheiropachys colon		
25	Dinotiscus bidentulus		
26	Braconid		
27	Anthocoris sarothamni		
28	Ilyobates nigricollis		
29	Gonioctena olivacea		
30	Phytodecta olivacea		
31	Exochomus quadripustulatus		
32	Propylaea quatuordecimpunctata		
33	Adalia decempunctata		
34	Adalia bipunctata		
35	Sitona regensteinensis		
36	Heterocordylus tibialis		
37	Philodromus aurelolus caespiticolis		
38	Linyphia triangularis		
39	Evarcha arcuata		
40	Xysticus cristatus		

Table A8

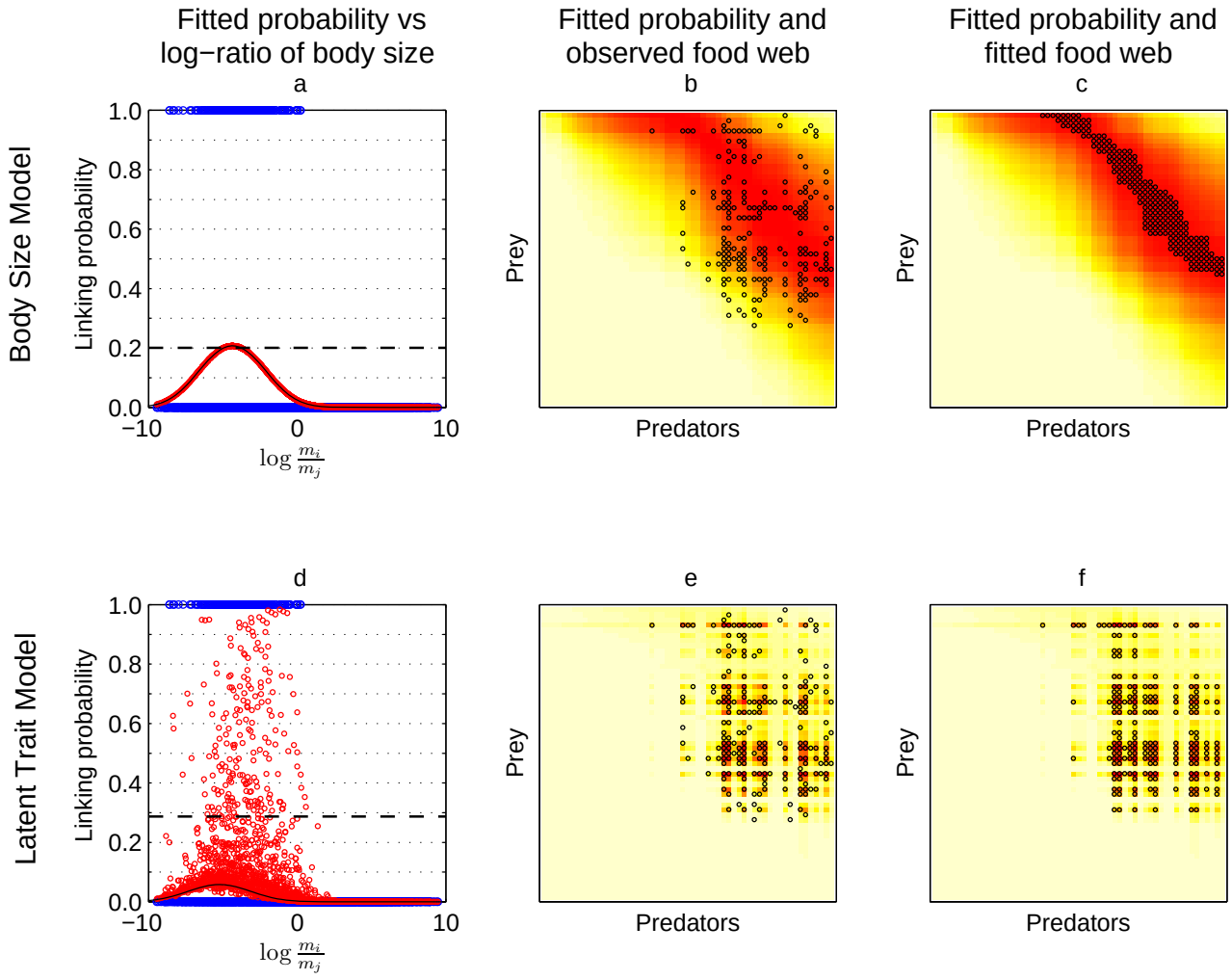

Figure A13: Celtic Sea

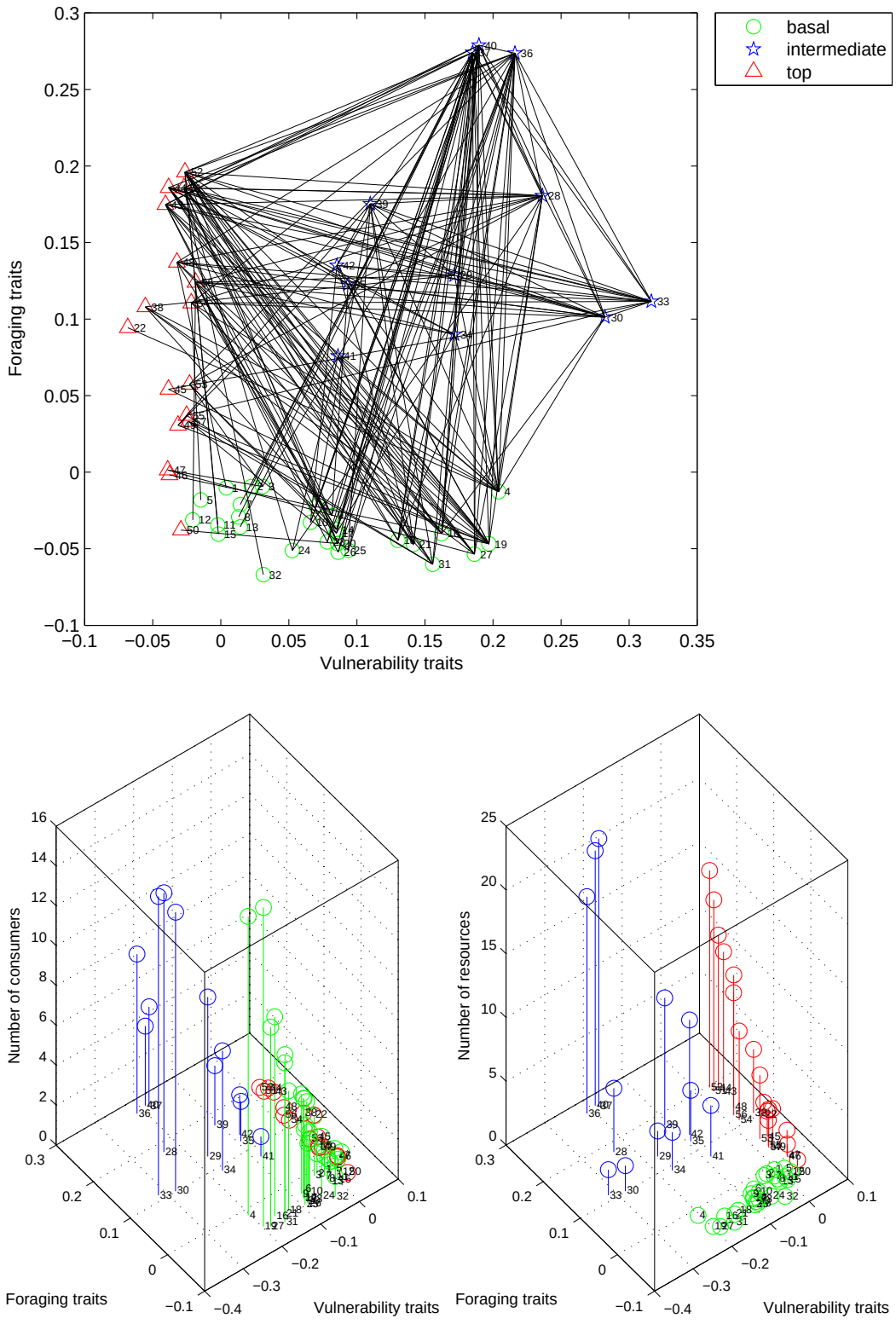

Figure A14: Celtic Sea

Celtic Sea			
Sp. no.	Species name	Sp. no.	Species name
1	Glyptocephalus cynoglossus	41	Trisopterus luscus
2	Fish-Larvae	42	Leucoraja naevus
3	Sandeel	43	Lophius budegassa
4	Goby	44	Zeus faber
5	Agonus cataphractus	45	Melanogrammus aeglefinus
6	Capros aper	46	Lepidorhombus boscii
7	Myctophid	47	Raja undulata
8	Gaidropsarus vulgaris	48	Squalus acanthias
9	Gadiculus argenteus	49	Leucoraja fullonica
10	Cepola macrophthalma	50	Galeorhinus galeus
11	Rockling	51	Lophius piscatorius
12	Hatchet-fish	52	Gadus morhua
13	Scaldfish	53	Raja montagui
14	Sprattus sprattus	54	Raja clavata
15	Buglossidium luteum	55	Molva molva
16	Trisopterus esmarkii	56	Pollachius virens
17	Clupeoid	57	Pollachius pollachius
18	Gadoid		
19	Callionymus lyra		
20	Hippoglossoides platessoides		
21	Microchirus variegatus		
22	Arnoglossus imperialis		
23	Argentina sphyraena		
24	Flatfish		
25	Engraulis encrasicolus		
26	Trisopterus		
27	Fish-unidentified		
28	Trisopterus minutus		
29	Micromesistius poutassou		
30	Trachurus trachurus		
31	Sardina pilchardus		
32	Microstomus kitt		
33	Scomber scombrus		
34	Clupea harengus		
35	Eutrigla gurnardus		
36	Merlangius merlangus		
37	Lepidorhombus whiffiagonis		
38	Chelidonichthys cuculus		
39	Scyliorhinus canicula		
40	Merluccius merluccius		

Table A9

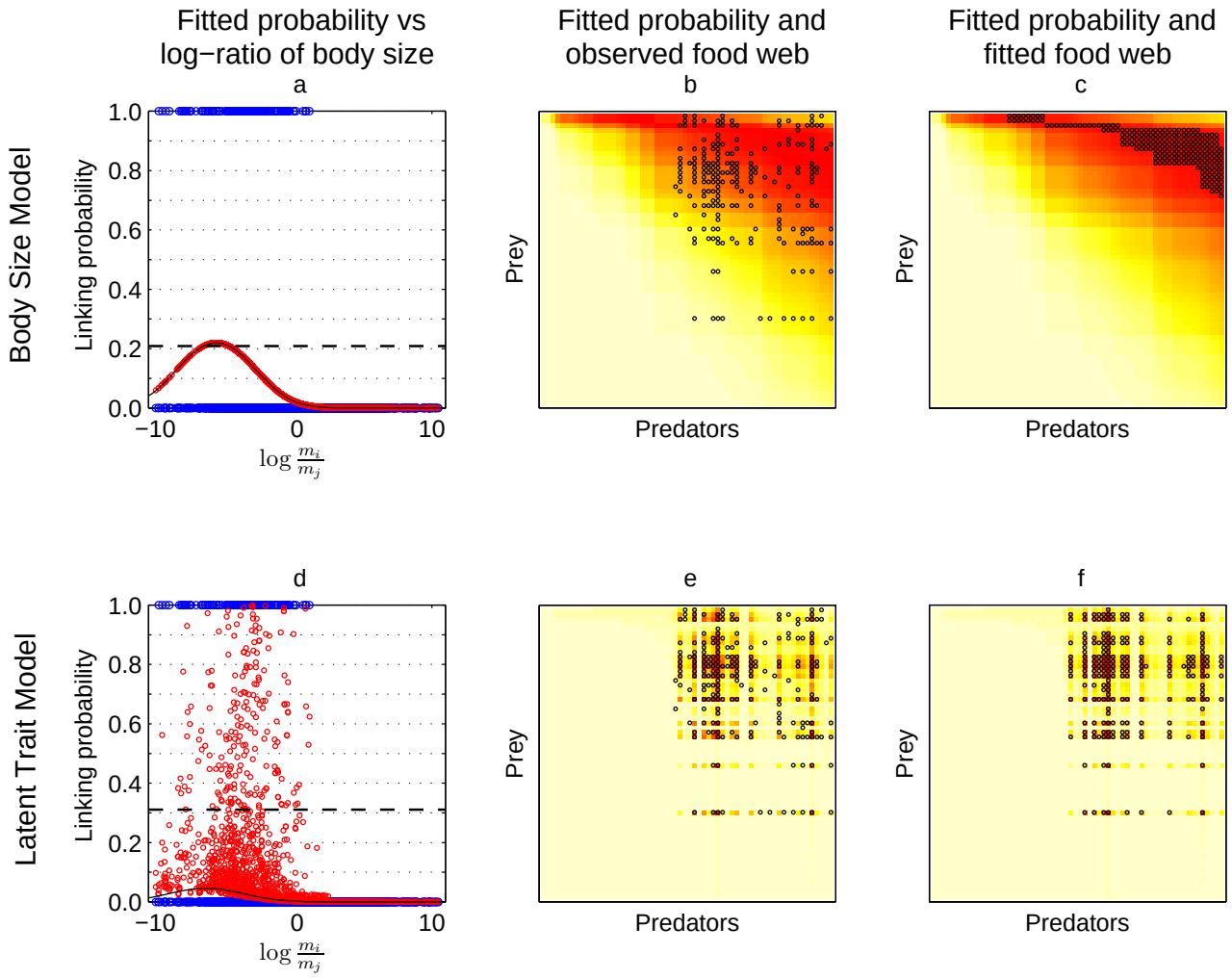

Figure A15: Mulgrave River

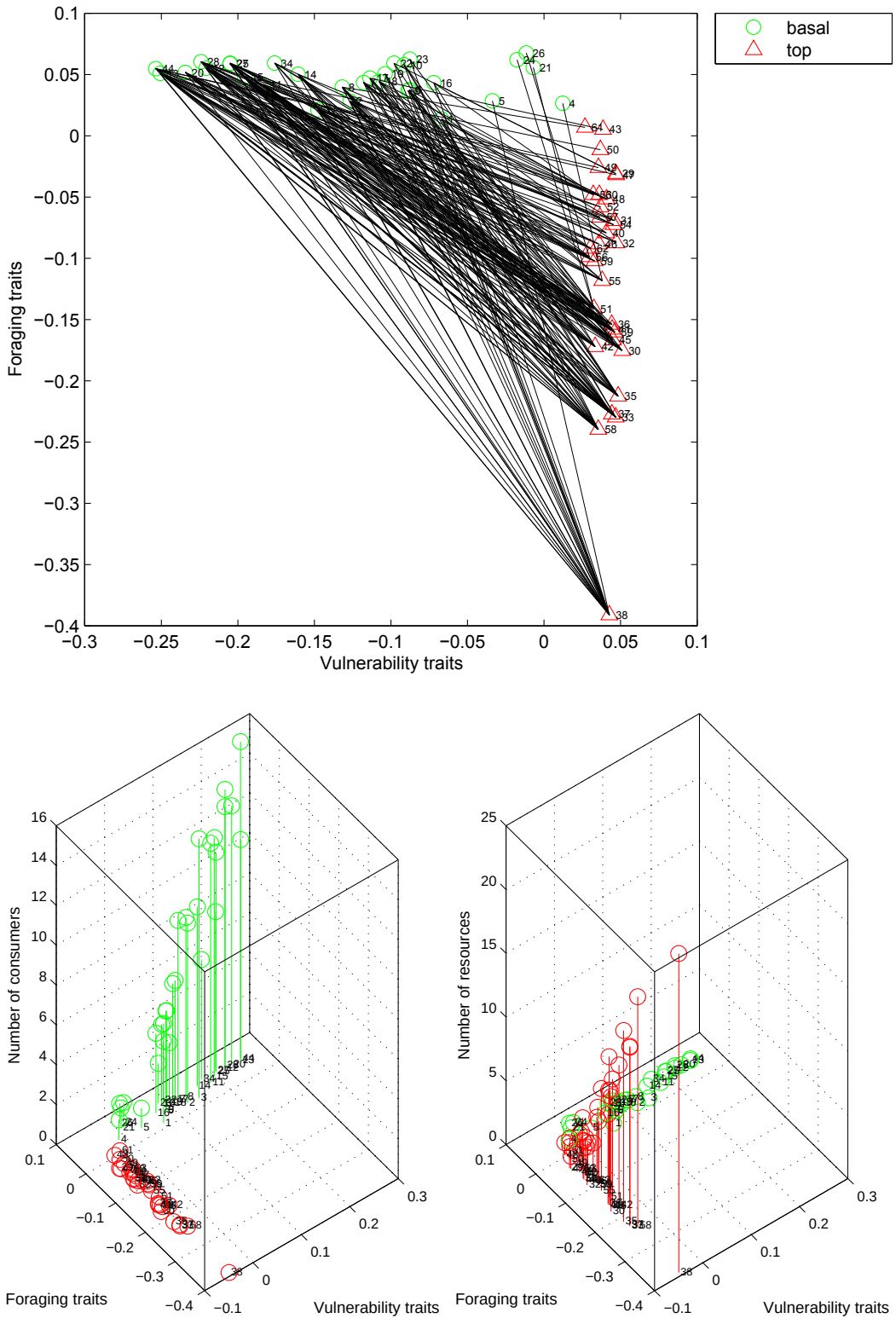

Figure A16: Mulgrave River

Mulgrave River			
Sp. no.	Species name	Sp. no.	Species name
1	Diatoms and desmids	41	Awaous acritosus
2	Filamentous algae	42	Gerres filamentosus
3	Detritus	43	Herring
4	Testate amoeba adults	44	Fish
5	Collembola juveniles	45	Giuris margaritacea
6	Diptera (not Chironomidae) larvae	46	Leiognathus equulus
7	Aquatic macrophytes	47	Caranx ignobilis
8	Elmidae larvae	48	Kuhlia rupestris
9	Hemiptera adults	49	Notesthes robusta
10	Arachnida adults	50	Microphis brachyurus
11	Diptera larvae	51	Hephaestus tulliensis
12	Ostracoda adults	52	Acanthopagrus berda
13	Chironomidae larvae	53	Arrhamphus sclerolepis
14	Corixidae and Notonectidae - incl. Plea adults	54	Lutjanus argentimaculatus
15	Ephemeroptera larvae	55	Nematalosa erebi
16	Small terrestrial inverts adults	56	Bunaka gyrinoides
17	Planktonic inverts - Cladocera etc adults	57	Anguilla reinhardtii
18	Hymenoptera adults	58	Neosilurus ater
19	Lepidoptera larvae	59	Tandanus tandanus
20	Trichoptera larvae	60	Mugil cephalus
21	Terrestrial vegetation	61	Anguilla australis
22	Gerridae and Mesovelioidea adults	62	Lates calcarifer
23	Large terrestrial inverts adults		
24	Fruit		
25	Decapoda adults		
26	Orthoptera adults		
27	Odonata larvae		
28	Mollusca adults		
29	Toxotes chatareus		
30	Redigobius bikolanus		
31	Xiphophorus maculatus		
32	Pseudomugil signifer		
33	Hypseleotris compressa		
34	Macrobrachium adults		
35	Ambassis agassizii		
36	Craterocephalus stercusmuscarum		
37	Glossamia aprion		
38	Melanotaenia splendida		
39	Tilapia mariae		
40	Glossogobius		

Table A10

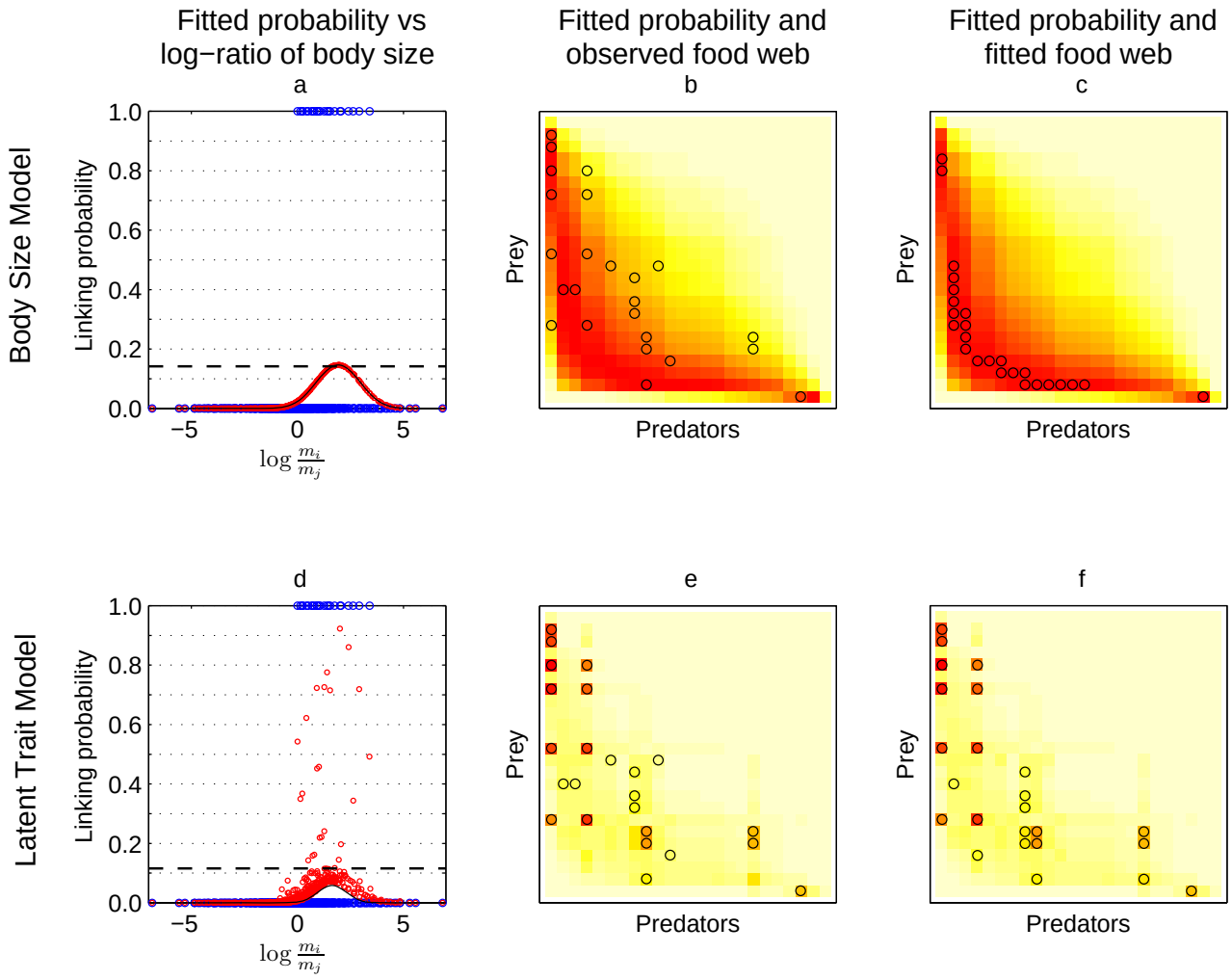

Figure A17: Goettingen

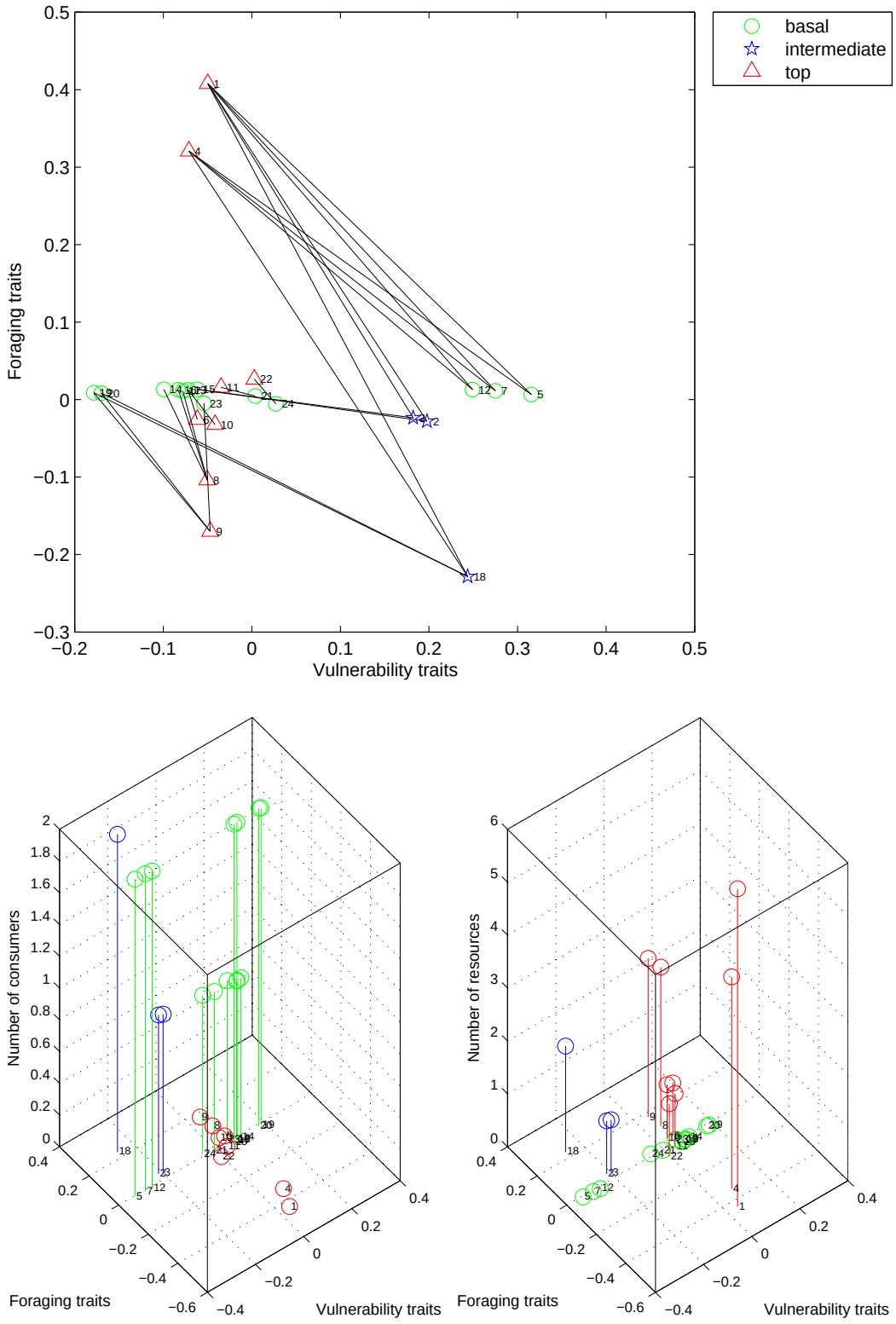

Figure A18: Goettingen

Goettingen	
Sp. no.	Species name
1	Basalys parva adults
2	Kleidotoma psiloides adults
3	Pentapleura adults
4	Idiotypa nigriceps adults
5	Aspilota (Species 2) adults
6	Alloxysta victrix adults
7	Aspilota (Species 5) adults
8	Ismarus dorsiger adults
9	Aspilota adults
10	Dendrocerus carpenteri adults
11	Pediobius foliorum adults
12	Aspilota (Species 3) adults
13	Aphidius ervi adults
14	Aphelopus holomelas adults
15	Limosina sp. pupae
16	Aphelopus melaleucus adults
17	Aphelopus serratus adults
18	Orthostigma adults
19	Megaselia pupae
20	Megaselia ruficornis pupae
21	Eulophus larvarum adults
22	Atractodes adults
23	Gymnophora arcuata pupae
24	Pegomya pupae

Table A11

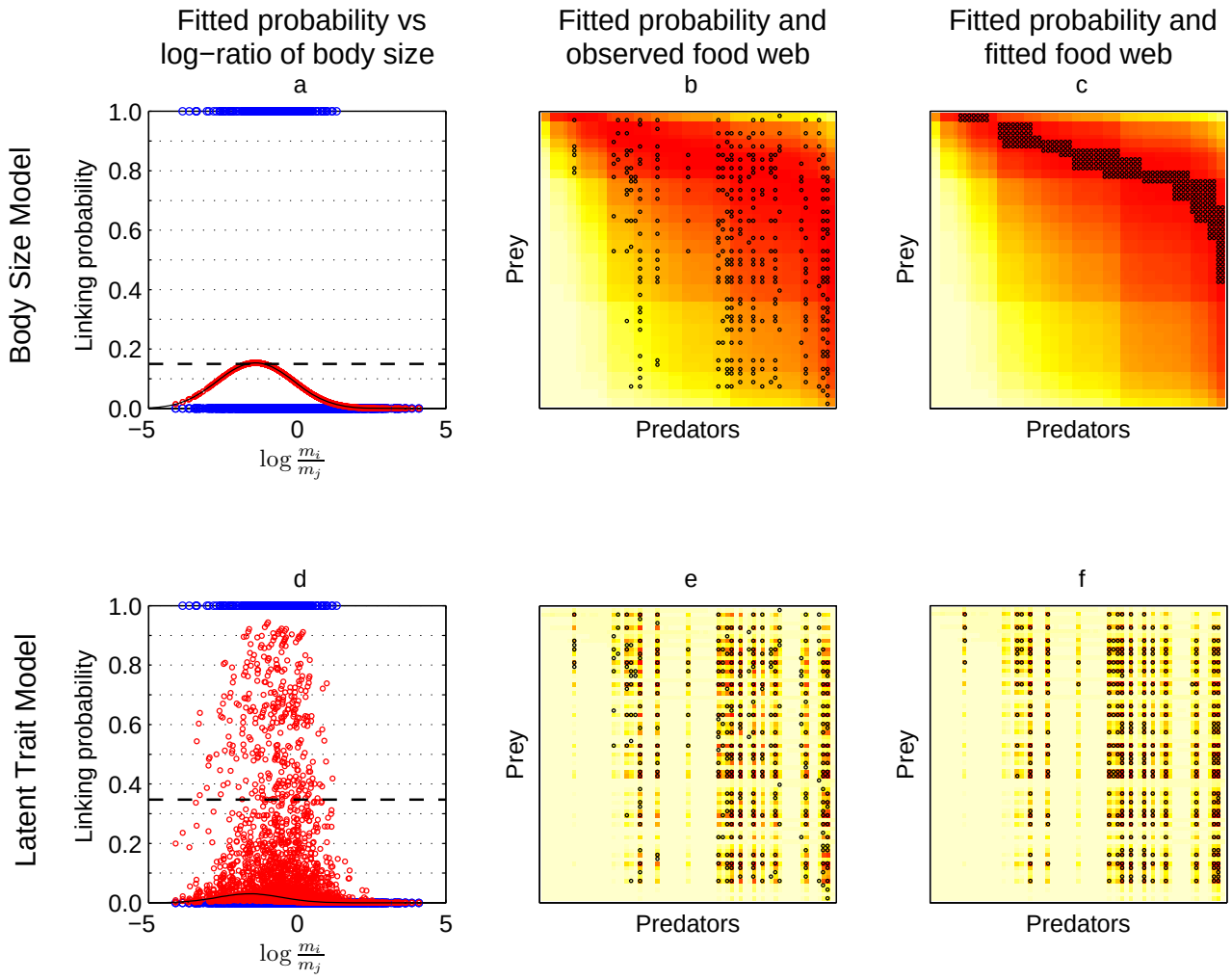

Figure A19: Skipwith

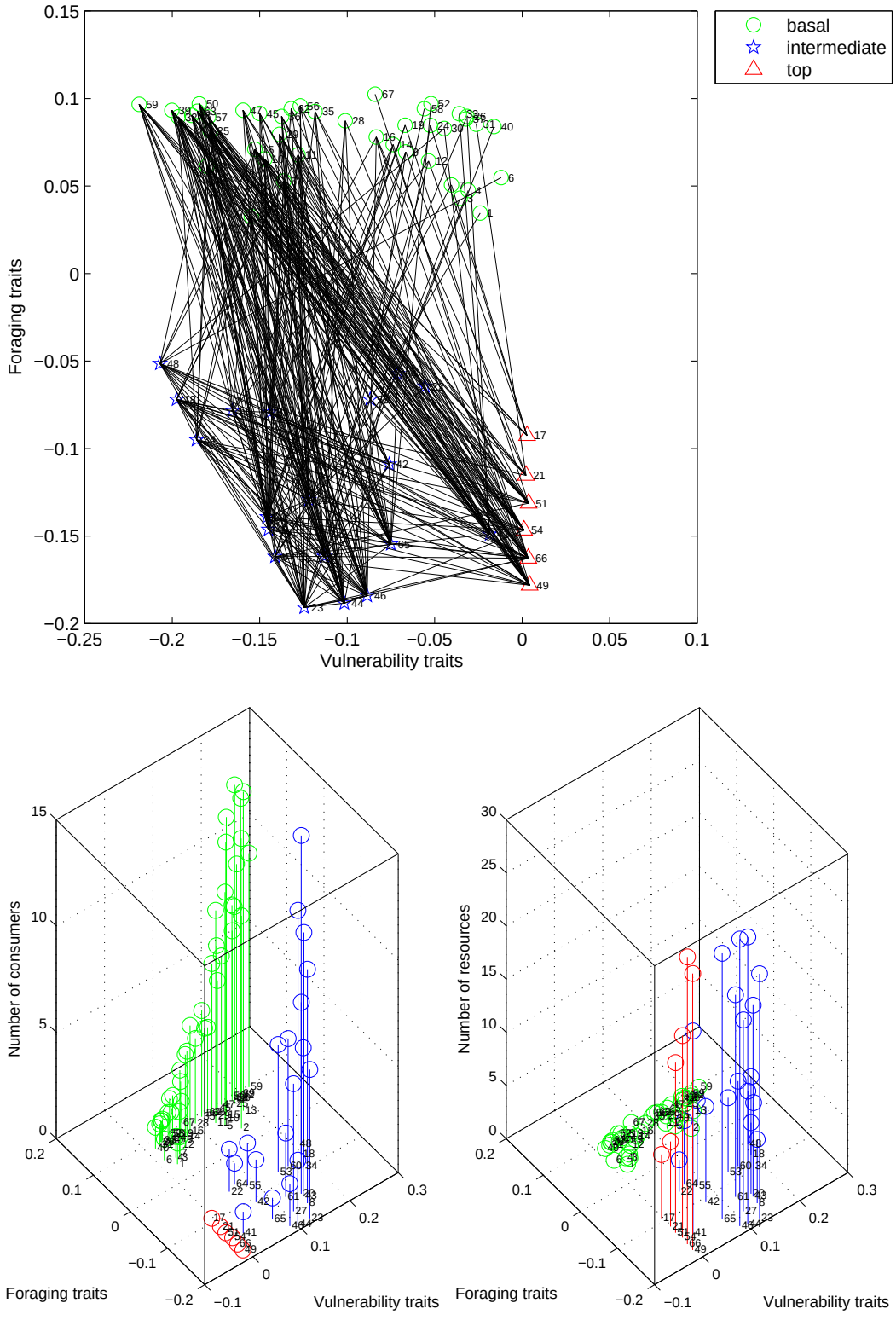

Figure A20: Skipwith

Skipwith			
Sp. no.	Species name	Sp. no.	Species name
1	Chydorus latus adults	41	Argyroneta aquatica larvae
2	Chydorus latus larvae	42	Agabus sturmii adults
3	Scapholeberis mucronata adults	43	Agabus sturmii larvae
4	Scapholeberis mucronata juveniles	44	Agabus bipustulatus adults
5	Scapholeberis mucronata larvae	45	Agabus bipustulatus larvae
6	Oribatei sp adults	46	Illybius fuliginosus adults
7	Acanthocyclops vernalis adults	47	Illybius fuliginosus larvae
8	Acanthocyclops vernalis larvae	48	Sialis lutaria larvae
9	Enchytraeidae adults	49	Lestes sponsa adults
10	Chironomidae larvae	50	Lestes sponsa larvae
11	Enchytraeidae larvae	51	Sialis lutaria adults
12	Corynoneura scutellata adults	52	Limnephilus marmoratus adults
13	Corynoneura scutellata larvae	53	Limnephilus marmoratus larvae
14	Tanytarsus adults	54	Sympetrum scoticum adults
15	Tanytarsus larvae	55	Sympetrum scoticum larvae
16	Chironomidae adults	56	Corixa punctata adults
17	Procladius sagittalis adults	57	Corixa punctata larvae
18	Procladius sagittalis larvae	58	Corixa dentipes adults
19	Hydroporus erythrocephalus adults	59	Corixa dentipes larvae
20	Hydroporus erythrocephalus larvae	60	Notonecta glauca larvae
21	Polycelis tenuis larvae	61	Notonecta glauca adults
22	Enallagma cyathigerum adults	62	Lumbriculus variegatus adults
23	Enallagma cyathigerum larvae	63	Lumbriculus variegatus larvae
24	Glyptotendipes pallens adults	64	Aeshna juncea adults
25	Glyptotendipes pallens larvae	65	Aeshna juncea larvae
26	Holocentropus picicornis adults	66	Dytiscus marginalis adults
27	Holocentropus picicornis larvae	67	Dytiscus marginalis larvae
28	Sigara semistriata adults		
29	Sigara semistriata larvae		
30	Chironomus dorsalis adults		
31	Chironomus dorsalis juveniles		
32	Chironomus dorsalis larvae		
33	Callicorixa praeusta adults		
34	Callicorixa praeusta larvae		
35	Hesperocorixa linnei adults		
36	Hesperocorixa linnei larvae		
37	Hesperocorixa sahlbergi adults		
38	Hesperocorixa sahlbergi larvae		
39	Arctocorisa germari larvae		
40	Argyroneta aquatica adults		

Table A12

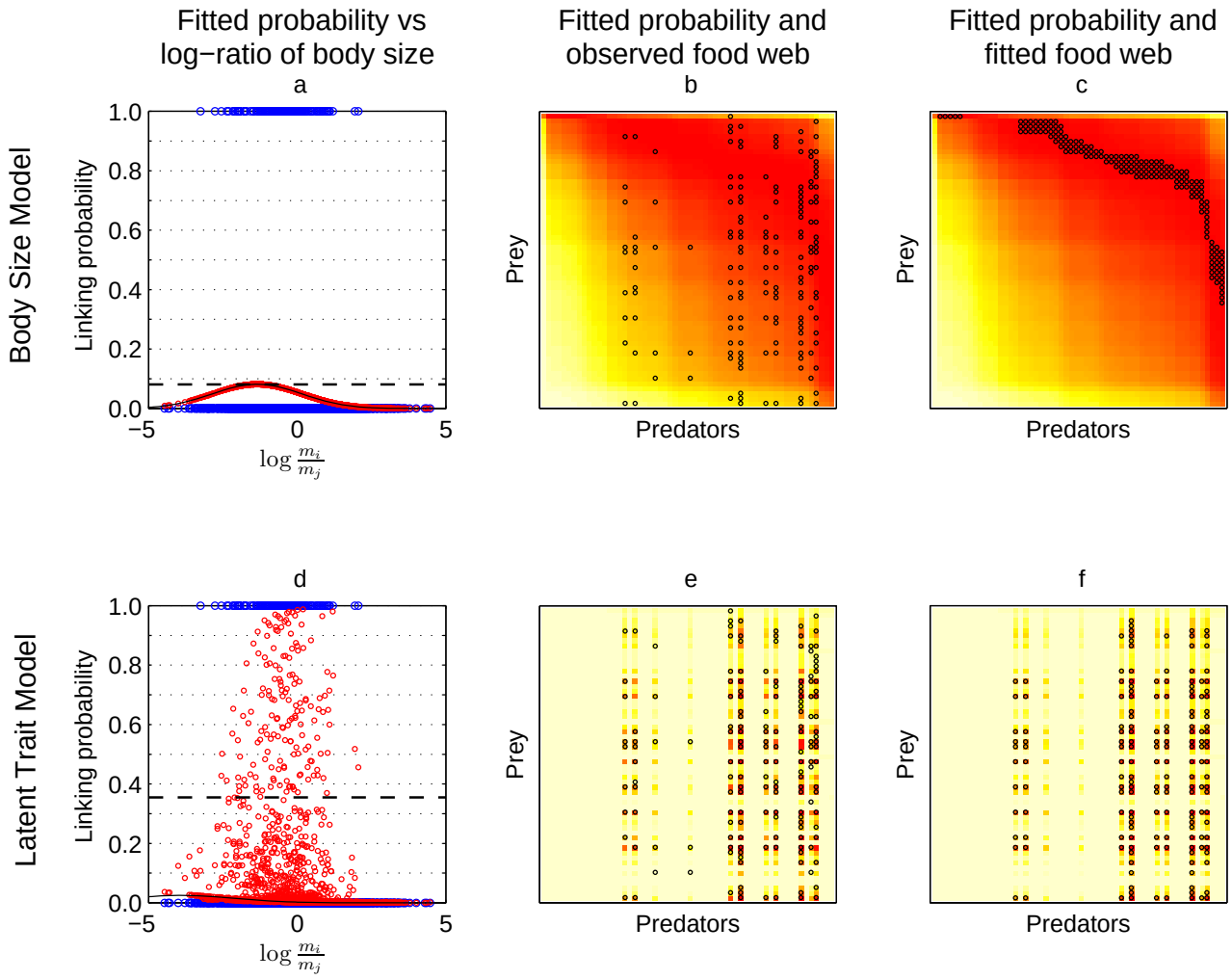

Figure A21: Sheffield

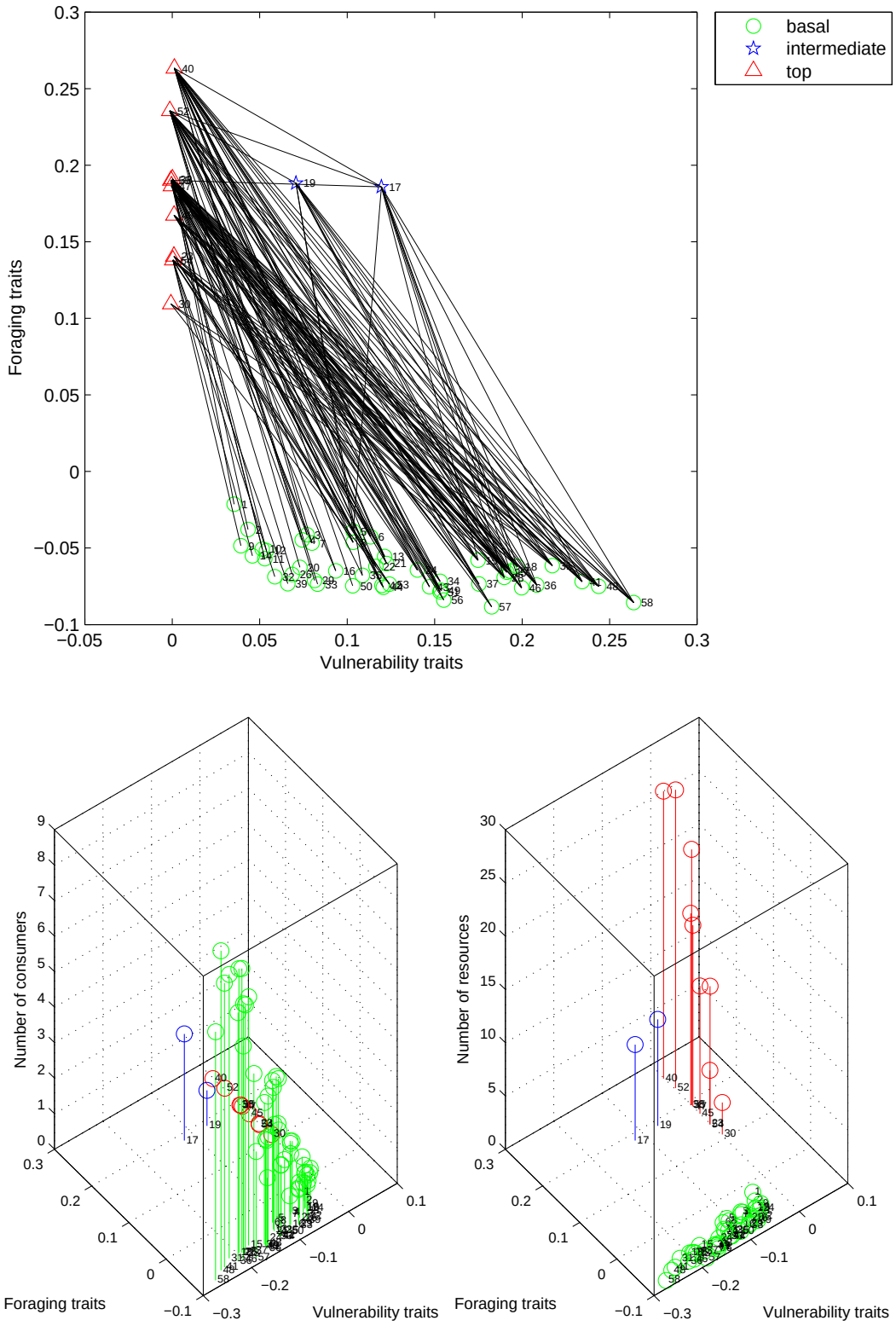

Figure A22: Sheffield

Sheffield			
Sp. no.	Species name	Sp. no.	Species name
1	Chydoridae (Species 1)	41	Ceratopogonidae
2	Lymnea	42	Limnephilus centralis
3	Acari (Species 1)	43	Limnephilus flavicornis
4	Cyclopoidea	44	Corixa punctata
5	Simocephalus vetulus	45	Sialis lutaria adults
6	Daphnia pulex	46	Chaoborus obscuripes
7	Acari (Species 2)	47	Agabus larvae
8	Ostracoda	48	Chironomidae (Species 1)
9	Caenis horaria	49	Chaoborus crystallinus larvae
10	Potamopyrgus jenkinsi	50	Chaoborus crystallinus pupae
11	Hygrotus inaequalis	51	Sialis lutaria
12	Haliplus ruficollis	52	Notonecta glauca adults
13	Polycelis tenuis	53	Tubificidae
14	Unionicola Pentatax	54	Cyrnus flavidus
15	Daphnia magna	55	Aeshna cyanea larvae
16	Hesperocorixa castanea	56	Sigara dorsalis larvae
17	Cymatia coleoptrata	57	Sigara nigrolineata
18	Cloeon dipterum	58	Tubificidae (Species 1)
19	Noterus clavicornis		
20	Laccophilus minutus		
21	Caenis luctuosa		
22	Helobdella stagnalis		
23	Helobdella stagnalis adults		
24	Nemoura cinerea		
25	Crangonyx pseudogracilis		
26	Lymnea peregra		
27	Chironomidae (Species 2)		
28	Culicidae		
29	Sigara dorsalis		
30	Polycelis tenuis adults		
31	Asellus aquaticus		
32	Ischnura elegans		
33	Agabus nebulosus		
34	Chironomidae (Species 3)		
35	Chironomidae (Species 5)		
36	Chironomidae (Species 4)		
37	Gammarus pulex		
38	Coenagrion puella larvae		
39	Piscicola geometra		
40	Agabus bipustulatus adults		

Table A13

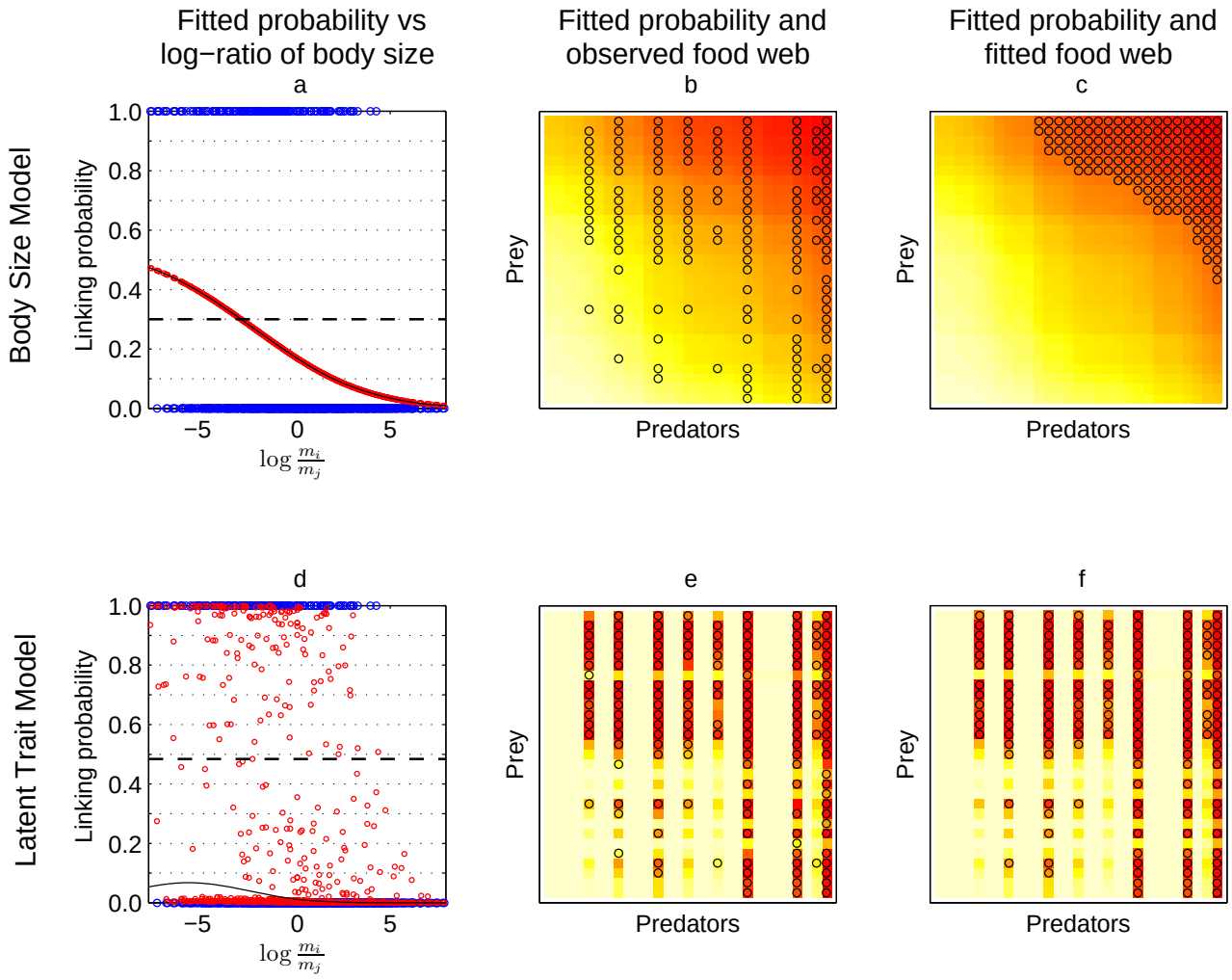

Figure A23: Broadstone Stream

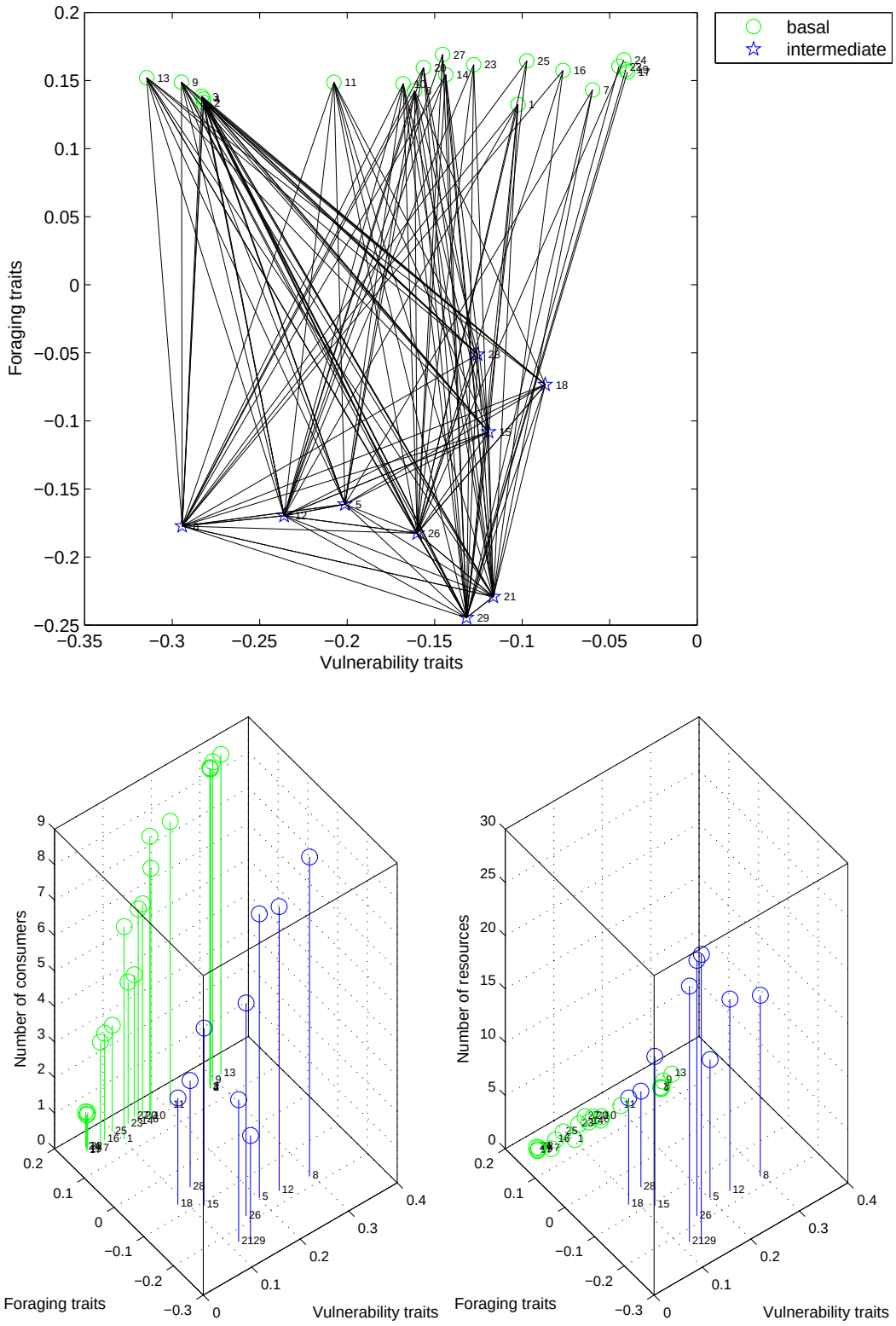

Figure A24: Broadstone Stream

Broadstone Stream			
Sp. no.	Species name	Sp. no.	Species name
1	Corynoneura lobata larvae	41	Argyroneta aquatica larvae
2	Micropsectra bidentata larvae	42	Agabus sturmii adults
3	Polypedilum albicorne larvae	43	Agabus sturmii larvae
4	Heterotrissocladius marcidus larvae	44	Agabus bipustulatus adults
5	Zavrelimyia barbatipes larvae	45	Agabus bipustulatus larvae
6	Brillia modesta larvae	46	Illybius fuliginosus adults
7	Paraleptophlebia submarginata larvae	47	Illybius fuliginosus larvae
8	Trissopelopia longimana larvae	48	Sialis lutaria larvae
9	Leuctra nigra larvae	49	Lestes sponsa adults
10	Simulium larvae	50	Lestes sponsa larvae
11	Nemurella pictetii larvae	51	Sialis lutaria adults
12	Macropelopia nebulosa larvae	52	Limnephilus marmoratus adults
13	Prodiamesa olivacea larvae	53	Limnephilus marmoratus larvae
14	Leuctra hippopus larvae	54	Sympetrum scoticum adults
15	Siphonoperla torrentium larvae	55	Sympetrum scoticum larvae
16	Niphargus aquilex adults	56	Corixa punctata adults
17	Diptera larvae	57	Corixa punctata larvae
18	Dicranota larvae	58	Corixa dentipes adults
19	Adicella reducta larvae	59	Corixa dentipes larvae
20	Oligochaeta larvae; adults	60	Notonecta glauca larvae
21	Plectrocnemia conspersa larvae	61	Notonecta glauca adults
22	Asellus meridianus adults	62	Lumbriculus variegatus adults
23	Tipulidae larvae	63	Lumbriculus variegatus larvae
24	Oligochaeta	64	Aeshna juncea adults
25	Scirtidae (previous Helodidae) sp. larvae	65	Aeshna juncea larvae
26	Sialis fuliginosa larvae	66	Dytiscus marginalis adults
27	Potamophylax cingulatus larvae	67	Dytiscus marginalis larvae
28	Pedicia larvae		
29	Cordulegaster boltonii larvae		
30	Chironomus dorsalis adults		
31	Chironomus dorsalis juveniles		
32	Chironomus dorsalis larvae		
33	Callicorixa praeusta adults		
34	Callicorixa praeusta larvae		
35	Hesperocorixa linnei adults		
36	Hesperocorixa linnei larvae		
37	Hesperocorixa sahlbergi adults		
38	Hesperocorixa sahlbergi larvae		
39	Arctocorisa germari larvae		
40	Argyroneta aquatica adults		

Table A14